The Shell Region of the Nucleus Ovoidalis: A Subdivision of the Avian Auditory Thalamus

SARAH E. DURAND, JAMES M. TEPPER, AND MEI-FANG CHENG
Institute of Animal Behavior (S.E.D., M.-F.C.) and Center for Molecular and Behavioral
Neuroscience (J.M.T.), Rutgers, The State University of New Jersey, Newark,
New Jersey 07102

ABSTRACT

The connectivity of a region surrounding the established thalamic auditory nuclei, n. ovoidalis (Ov) and n. semilunaris parovoidalis (SPO), was explored in the ring dove by using the anterograde tracers, *Phaseolus vulgaris* leucoagglutinin (PHAL) and biocytin, and the retrograde tracer, fluorogold. The Ov-SPO surround received a projection from a cell group along the interface of the auditory midbrain and the n. intercollicularis, as revealed with PHAL and biocytin, and was composed of neurons exhibiting a common morphology. These features and the presence of overlapping projections from different portions of the Ov-SPO surround suggest that this region comprises a functionally discrete area, which we term the Ov shell. Single unit recording within the shell established the existence of acoustically responsive units.

Both PHAL and fluorogold labeling revealed a robust projection from the Ov shell to the caudomedial hypothalamus. Major telencephalic projections of the shell terminated within the ventral paleostriatal complex, "end-zones" of the field L, the caudomedial hyperstriatum ventrale, and regions immediately dorsal and lateral to the auditory neostriatum. Except for a portion of the shell bordering medial ovoidalis, PHAL injections into the shell also labeled fibers within the caudolateral neostriatum and along the lateral neostriatal rim.

The connectivity of the Ov shell suggests that this region may integrate auditory pathways with brain regions associated with endocrine mediated behavior. In addition, the shell may constitute a source of converging input to several levels of central auditory pathways. © 1992 Wiley-Liss, Inc.

Key words: PHAL, extracellular recording, acoustic stimuli, hypothalamus, ring dove

The classic studies of Karten ('67, '68) that established the nuclei ovoidalis (Ov) and semilunaris parovoidalis (SPO) as the avian auditory thalamus and the neostriatal Field L of Rose (Rose, '14) as its target also described unconfirmed projections from the auditory thalamus to the lateral neostriatum caudale, to the paleostriatum, and to other cell groups. The presence of thalamic auditory fields in these additional cell groups remained unconfirmed, and there have been few attempts to subdivide the avian auditory thalamus on the basis of afferentation and cytoarchitecture. The auditory thalamus has been frequently presented as synonymous with the nucleus ovoidalis, which has been ascribed a relatively simple organization and the relatively circumscribed function of a relay center for midbrain auditory input to the caudomedial neostriatum (Bonke et al., '79a; Kelley and Nottebohm, '79; Bigalke-Kunz et al., '87; Hausler, '88).

Recent evidence has begun to reveal the complexity of the auditory thalamus in birds. The afferent and efferent connectivity of SPO is now recognized as distinct from Ov (Wild, '87a; Wild et al., '90). Studies in the pigeon (*Columba livia*) have demonstrated that SPO receives lemniscal afferents (Ov does not) and projects to an "end-zone" of the auditory neostriatum, L_{2b}, that is dorsolateral to the major (L_{2a}) and minor (L_1 and L_3) terminal fields of Ov (Bonke et al., '79a; Fortune and Margoliash, '91).

In the budgerigar (*Melopsittacus undulatus*), Ovm, a distinct area immediately ventral and medial to Ov, receives midbrain auditory afferents and projects to both field L and to a laterally adjacent neostriatal field (Brauth et al., '87). The passerine Ovm, studied in the zebra finch (*Poephila guttata*), projects to L_{2b}, the target of SPO in the pigeon (Fortune and Margoliash, '91). Homologies between the budgerigar and zebra finch Ovm remain unclear. However, all three of the recent studies cited above describe a portion of the Ov surround, whether SPO or Ovm, that projects to

an end-zone of the primary projection of Ov (Wild et al., '90; Fortune and Margoliash, '91).

Other portions of the Ov surround have been also implicated in ascending auditory pathways. Injections of retrograde tracer into discrete regions of field L in the starling (*Sternus vulgaris*) labeled some cells within the *lateral* and ventral Ov surround (Hausler, '88), which included the proximal portion of the tractus nuclei ovoidalis (TOv). Fortune and Margoliash ('91) have reported that neurons within TOv project caudally to L_2. In sum, regions peripheral to Ov have been identified as projecting to regions caudal, lateral, and dorsal to the terminal fields of Ov neurons. Not all identified cell groups have been described within a single species and only one, SPO, has been demonstrated to receive a unique projection from ascending auditory pathways.

A recent study by Brauth and Reiner ('91) has distinguished biochemically a subdivision of the auditory thalamus that exists in birds (the pigeon) and in other vertebrate groups. Neurons along the circumference of Ov, and scattered within SPO and peri-Ov regions lateral and dorsal to SPO, were found to contain calcitonin-gene related peptide. Axons containing this peptide innervated all zones of field L. Also labeled was a region along the third ventricle that extended dorsally and laterally from field L into a region previously identified as its target and designated the neostriatum dorsale (Bonke et al., '79a; Wild et al., '90). This labeled periventricular zone of the neostriatum was continuous with lightly labeled tissue in the medially adjacent hyperstriatal periventricular zone, which had not been previously implicated as part of central auditory pathways.

No descending projections from the avian auditory thalamus have been previously reported. However, regions of the thalamus that receive input from the auditory midbrain have been shown to project to the hypothalamus in both mammals and amphibians (LeDoux, '85; Neary and Wilcznski, '86). Behavioral and physiological data for all three vertebrate classes have suggested that species-specific vocalizations have a stimulatory effect upon gonadal function. In birds and mammals, male vocalizations performed during courtship have been shown to stimulate ovulation (Kroodsma, '76; McComb, '87). In amphibians, the male's mating call stimulates testicular androgen production (Brzoska and Obert, '80) and acoustically responsive units have been recorded in the amphibian ventral hypothalamus (Wilczynski and Allison, '89) and anterior preoptic nucleus (Urano and Gorbman, '81).

The deafening of female ring doves (*Streptopelia risoria*), birds that vocalize for extended periods during courtship, has been demonstrated to delay egg-laying (Nottebohm and Nottebohm, '71). Both auditory and proprioceptive components of the female's performance of courtship vocalizations have been found to enhance her gonadotropin levels (Cohen and Cheng, '79, '81; Cheng, '86; Cheng et al., '88). In the budgerigar, hearing conspecific courtship vocalizations is necessary for the maintenance of mature gonadal function in both sexes (Brockway, '69). These observations suggest that birds may also possess direct thalamic auditory pathways to the hypothalamus.

The posteromedial hypothalamus is essential to estrogen-dependent courtship in female ring doves (Gibson and Cheng, '79). This region projects upon the nucleus intercol-

Abbreviations

AA	archistriatum anterior	NC	neostriatum caudale
AI	archistriatum intermedium	NCl	neostriatum caudale, pars lateralis
AIv	archistriatum intermedium, pars ventralis	NCm	neostriatum caudale, pars medialis
AL	ansa lenticularis	NI	neostriatum intermedium
AM	n. anterior medialis hypothalami	OM	tractus occipitomesencephalicus
AP	area pretectalis	Ov	n. ovoidalis
BO	bulbus olfactorius	Ov*	Ov shell, where * = a (anterior), p (posterior), l (lateral),
CA	commissura anterior		m (medial)
CIO	capsula interna occipitalis	PA	paleostriatum augmentatum
CO	chiasma opticum	PMl	n. paramedianus
CP	commissura posterior	POM	n. preopticus medialis
DIP	n. dorsointermedius posterior thalami	PP	paleostriatum primitivum
DLA	n. dorsolateralis anterior thalami	PTB	n. pretectalis
DLP	n. dorsolateralis posterior thalami	PV	paleostriatum ventralis
DMP	n. dorsomedialis posterior thalami	PVN	n. paraventricularis magnocellularis
EZ	end zone (of Ov shell)	Rt	n. rotundus
FPL	fasciculus prosencephali lateralis	SAC	stratum album centrale
GCt	substantia grisea centralis	SCE	stratum cellulare externum
HA	hyperstriatum accessorium	SGP	stratum griseum periventriculare
Hb	n. habenularis	SHL	n. subhabenularis lateralis
HL	n. habenularis lateralis	SHM	n. subhabenularis medialis
HV	hyperstriatum ventrale	SMe	stria medularis
ICo	n. intercollicularis	SL	n. septalis lateralis
IH	n. inferioris hypothalami	SM	n. septalis medialis
IN	n. infundibuli hypothalami	SPO	n. semilunaris parovoidalis
L_1, L_2, L_3	auditory neostriatum, zones 1, 2 and 3	SPC	n. superficialis parvicellularis
L_2v	ventromedial end-zone of L_2	SRt	n. subrotundus
LFS	lamina frontalis superior	T	n. triangularis
LH	lamina hyperstriatica	Tn	n. taeniae
LHy	regio lateralis hypothalami	TO	tuberculum olfactorium
LMD	lamina medullaris dorsalis	TOv	tractus nuclei ovoidalis
LPO	lobus parolfactorius	TSM	tractus septomesencephalicus
MLd	n. mesencephalicus lateralis, pars dorsalis	TTS	tractus thalamostriaticus
N	neostriatum	TPO	area temporo-parieto-occipitalis
Nd	neostriatum dorsale	V	ventriculus
Nl	neostriatum lateralis	VMN	n. ventromedialis hypothalami
NIII	nervus oculomotorius		

licularis (Berk and Butler, '81), an estrogen concentrating region of the tectum (Martinez-Vargas et al., '76) that specifically mediates the courtship vocalization (Cohen and Cheng, '81). The nucleus intercollicularis, in turn, projects upon regions that mediate gonadotropin secretion (Akesson et al., '87). Thus, should the avian posteromedial hypothalamus receive auditory afferents, a putative pathway exists whereby acoustic input could directly influence both the performance of courtship vocalizations and, indirectly, gonadotropin secretion.

Given evidence that the avian auditory thalamus is a potential source of auditory input to "subcortical" regions and to telencephalic fields peripheral to field L, this study explores these issues by examining the extent and connectivity of the avian auditory thalamus in the ring dove using anterograde and retrograde tract tracing and extracellular recording. Portions of this work have been previously presented in abstract form (Durand et al., '89, '90).

MATERIALS AND METHODS
Animals

Thirty-two ring doves of both sexes, aged 4 months to 3 years, and bred at the Institute of Animal Behavior at Rutgers, were used for the anatomical studies; 16 birds were subjects for anterograde tracing experiments with *Phaseolus vulgaris* leucoagglutinin (PHAL) and 4 received injections of the anterograde tracer biocytin (King et al., '89; Izzo, '91). Four injections of PHAL were made into Ov proper and eight into regions of the Ov-SPO surround. An additional four birds received midbrain injections along the medial interface of the nucleus mesencephalicus lateralis (MLd) and the nucleus intercollicularis (ICo). Biocytin injections were delivered into portions of MLd or ICo that were adjacent to the interface zone. Seven birds received injections of the retrogradely transported dye fluorogold into putative targets of the auditory thalamus. An additional five birds were used for electrophysiological examination of single and multi-unit responses to acoustic stimuli within regions surrounding Ov. All birds were reared in 2.5' × 2' × 1.5' breeding cages and subsequently housed in groups of 3–5 in large stock cages, when not paired for breeding. Water, a seed mixture and vitamin enriched gravel were provided *ad libitum*.

Anterograde tracing

Doves were anesthetized with a mixture of chloral hydrate (64.0 mg/ml), sodium pentobarbital (32.1 mg/ml), and magnesium sulfate (13.7 mg/ml) after a recipe provided by Fort Dodge Labs (formerly marketed as "Chloropent") at 2.5 ml/kg i.m. For injections into the auditory thalamus, the bird's head was held in an upright position, as specified by the atlas of Vowles et al. ('75) for the ring dove, and was fixed by a clamp that gripped the skull at a groove within the rostral aspect of the orbit. This head angle was initially chosen to facilitate concurrent unit recording experiments in the thalamus (see Electrophysiology). For injections into the midbrain, the bill was clamped to a David Kopf pigeon adaptor that was mounted on a 45° angled plate, as described in a previous study (Akesson et al., '87). Target coordinates for central Ov were 0.3 mm posterior to the interaural line (AP = −0.3), 0.8 mm lateral to the midline (ML = 0.8), and 6.4 mm ventral to the surface of the brain (DV = 6.4). Target coordinates for the medial MLd-ICo

interface were AP = −1.15, ML = 3.2, and DV = 6.3. A local anesthetic (2% lidocaine) was injected s.c. under the scalp once the bird was placed in the stereotaxic instrument. A midline incision exposed the skull and a small burr hole was drilled over the target region.

Glass micropipettes were cut back to tip diameters of 6–25 μm and filled with a 2.5% solution of PHAL (Vector Laboratories, Inc., Burlingame, CA) in 10 mM phosphate-buffered saline (pH 8.0) or a 5% solution of biocytin in 1.0 M potassium acetate. For eight PHAL injections into the thalamus and a single biocytin injection into MLd, the micropipette was initially used to record multi-unit responses to acoustic stimuli, in order to localize Ov (or MLd) prior to injections of the tracer into specific regions of the nucleus. After lowering the pipette to within 1 mm of the target under stereotaxic guidance, computer generated 500 ms white noise bursts (2/s at 75 dB SPL) were fed to a loudspeaker placed 0.5 m in front of the bird. Neural activity was amplified and displayed on one channel of a dual-beam oscilloscope, with the other channel displaying the acoustic stimulus. Once a strong response to the stimulus was observed, the pipette was withdrawn until a minimum but still detectable response was obtained. This depth was judged as the dorsal boundary of Ov (or MLd). The pipette was then positioned as desired for the experiment before delivering the PHAL (or biocytin) by iontophoresis (3.5–5.0 μA, 7 seconds on/off). Injection times of 13–20 minutes were used for PHAL and 30–40 minutes for biocytin. Following removal of the pipette, the wound was sutured, treated with an antiseptic (10% povidone-iodine), and the bird was returned to its home cage.

PHAL cases. Survival times varied between 10 and 15 days, with the longer times chosen to ensure adequate transport of the tracer to potentially distant projection sites. Transcardial perfusion was performed under deep Chloropent anesthesia with 50 ml of cold saline followed by a two-step fixative of 150 ml of 4% paraformaldehyde in 0.15 M sodium acetate buffer, pH 6.5, and 350 ml of 4% paraformaldehyde and 0.2% glutaraldehyde, in 0.15 M sodium borate buffer, pH 10.5. The brains were immediately removed from the skull, blocked at the angle of the Karten and Hodos ('67) atlas for the pigeon, and placed in the second fixative for overnight post-fixation at 4°C. If sections were to be cut on a freezing microtome, the brains were transferred to a solution of 20% sucrose in 0.15 M phosphate-buffered saline (pH 7.4) for 48 hours at 4°C prior to sectioning. Otherwise, sections were cut on a Vibratome. Sections of 50 μm were collected in a chilled potassium phosphate-buffered saline (KPBS) containing 2% normal rabbit serum (NRS) and were incubated overnight at 4°C in 0.3% Triton X-100 under gentle rotation. The KPBS/NRS (or KPBS) buffer was used throughout the following procedure for washes between incubations and for generating solutions. Sections were transferred to a 1:3,500 dilution of goat anti-PHA-L+E (Vector Laboratories, Inc.) for 48 hours at 4°C under gentle rotation. The tissue was then processed for immunoperoxidase staining according to the ABC method (Hsu et al., '81) with the Vectastain kit (Vector Laboratories, Inc.). At room temperature, sections were washed and incubated for 1 hour in a 1:200 dilution of biotinylated rabbit anti-goat antibody, washed again and then incubated with the avidin biotin peroxidase complex for 90 minutes. Sections were then washed and incubated at room temperature for 90 minutes in a solution of 0.05% 3,3'-diaminobenzidine (DAB), 0.05% glucose oxidase (Sigma

Chemical Co., St. Louis, MO), 0.04% ammonium chloride, and 0.2% β-d-glucose (Itoh et al., '79). After staining, the tissue was washed, mounted onto gelatin coated slides, air dried, and counterstained with either neutral red or cresyl violet prior to dehydration, clearing, and mounting in synthetic resin (Eukitt) under glass cover slips.

For midbrain injections and injections into the rostral and caudal aspects of the Ov surround, the tissue was processed following the Vector Laboratories protocol for PHAL localization (after Gerfen and Sawchenko, '84). Incubations with the secondary antibody and ABC complex were repeated prior to reacting with DAB. Sections from midbrain injections were nickel-intensified according to the glucose oxidase-DAB-nickel (GDN) method (Shu et al., '88); 2.5% nickel ammonium sulfate was included in the DAB solution, which was made with buffered 0.1 M potassium acetate, pH 6.0, in place of KPBS. Nickel-intensified sections were not counterstained because of background labeling that revealed fiber tracts and nuclei.

Biocytin cases. Four injections were made into the midbrain with biocytin (Sigma Chemical Co., St. Louis, MO) for the purpose of localizing precisely the source of the midbrain projection to the peripheral auditory thalamus; biocytin yielded better labeling of cell bodies and dendrites than did PHAL when small injection sites (100–200 μm diameters) were desired (King et al., '89). Iontophoresis of this tracer for 30 minutes as described above resulted in smaller and more discrete injection sites relative to what was obtained with PHAL. After a survival time of 30 hours, birds were sacrificed as above and transcardially perfused with 50 ml chilled buffered saline followed by 300 ml of 1% glutaraldehyde and 3% paraformaldehyde. Brains were blocked at the angle of the Karten and Hodos atlas ('67), removed from the skull, and immediately sectioned on a Vibratome. The vibratome-sectioned tissue was collected in chilled KPBS and incubated overnight at 4°C under gentle rotation in Vector's ABC complex with 0.6–1.0% Triton. The following day the tissue was washed in 0.1 M sodium acetate buffer, pH 6.5, and then stained by the GDN method. Neutral red was used as a counterstain.

Retrograde tracing

Two "subcortical" regions that were identified as targets of the auditory thalamus with PHAL, the medial hypothalamus and ventral paleostriatum, were selected for confirmation by retrograde transport, given the absence of any data regarding auditory projections to these regions in birds.

Seven birds received pressure injections of 5% fluorogold (Fluorochrome, Inc.) in distilled H_2O delivered with a 1 μl Hamilton syringe with an etched tip. Injections were delivered with the bird's head positioned according to the atlas for the ring dove (Vowles et al., '75), which ensured that the syringe needle would pass rostral to the auditory thalamus in all cases. Injections were made into the posterior hypothalamus (AP = +1.7, ML = 0.3) in three birds, two in the ventromedial (DV = 8.8) and one in the dorsomedial (DV = 8.4) region. Three birds received injections into the paleostriatal complex: the ventral paleostriatum (AP = +1.4, ML = 1.4, DV = 4.5) in one case and the lobus parolfactorius (AP +3.7, ML = 0.6, DV = 4.0) in two cases. In one bird, fluorogold was injected into the septum (AP = +1.4, ML = 0.5, DV = 4.9) in order to control for some diffusion of the tracer into this nucleus from the injection into the ventral paleostriatum.

Volumes of tracer injected were 0.15–0.20 μl for injections into the paleostriatal complex, septum, and dorsomedial hypothalamus and 0.07 μl for injections into the caudal ventromedial hypothalamus. Ten minutes after positioning the syringe, the fluorogold solution was injected at a rate of 0.01 μl per minute. Another 10 minute waiting period was observed before withdrawal of the syringe. Following a survival period of 7–10 days, birds were sacrificed and perfused with 50 ml of chilled saline, followed by 300 ml of 4% paraformaldehyde and 0.1% glutaraldehyde in 0.1 M phosphate buffer, pH 7.4. Brains were sectioned on a freezing microtome and immediately mounted onto slides. In most cases, every third section was counterstained with cresyl violet.

Electrophysiology

Birds were anesthetized with urethane (1.6 g/kg, i.m.). Additional injections were given i.p. when necessary, at 10% of the initial dose, during protracted recording sessions. The subject was loosely wrapped in a towel and placed in a Kopf small animal stereotaxic device equipped with sharp angled atraumatic ear bars. A topical anesthetic (2% lidocaine) was injected under the scalp prior to removal of the head feathers and exposure of the skull. An opening in the skull (approx. AP +1.0–AP −1.5, ML 0.5–ML 1.5) was drilled over the thalamus of the right hemisphere and the wound covered with bone wax. Two small flat-headed screws were affixed with cyanoacrylate glue and dental cement head down to the skull overlying the left hemisphere. Once the cement had hardened, the bird was removed from the stereotaxic instrument and the ears were inspected for any damage under a stereomicroscope. A thin metal plate, molded to fit the skull over the left hemisphere and attached to a conventional electrode carrier, was then secured to the bird's head by means of the skull screws, thereby freeing the ears from obstruction and stabilizing the head for electrophysiological recording. The bone wax was then removed.

Extracellular single unit and multi-unit recordings were obtained with glass micropipettes pulled from 2.0 mm (o.d.) capillary glass (WPI) on a Narishige vertical puller. They were filled with a 2% solution of Pontamine Sky Blue (PSB) (ICN Biomedicals) in 3 M NaCl and had tip diameters of 1–1.5 μm and in vivo impedances of 6–11 MΩ. Signals were amplified with a Neurodata IR183 preamplifier and displayed, together with acoustic stimuli, on a Tektronix 5110 storage oscilloscope. Data were stored on magnetic tape for off-line analysis by two programs (Scope and Spike Train), designed by one of us (J.M.T.), in conjunction with the following hardware: spike trains and any associated acoustic stimuli were acquired on a National Instruments NB-MIO 16L multifunction board and a Macintosh IIx computer. Wave forms were acquired and analyzed with a Nicolet 4094C digital oscilloscope linked to the computer via a National Instruments NB-GPIB board. Single units were discriminated by the amplitudes and waveforms of action potentials.

Recording was conducted in a sound insulated chamber and acoustic stimuli were generated by the SoundEdit (Farallon) program on a Macintosh IIx computer. The signals were delivered to a Yamaha NS 10M loudspeaker. Thalamic regions surrounding Ov were explored for acoustically responsive units with search stimuli consisting of 500 ms "white" noise bursts with a bandwidth of 0 to 11 kHz. Stimuli were delivered at 70 dB SPL once every 2 seconds. Once an auditory response was observed, spontane-
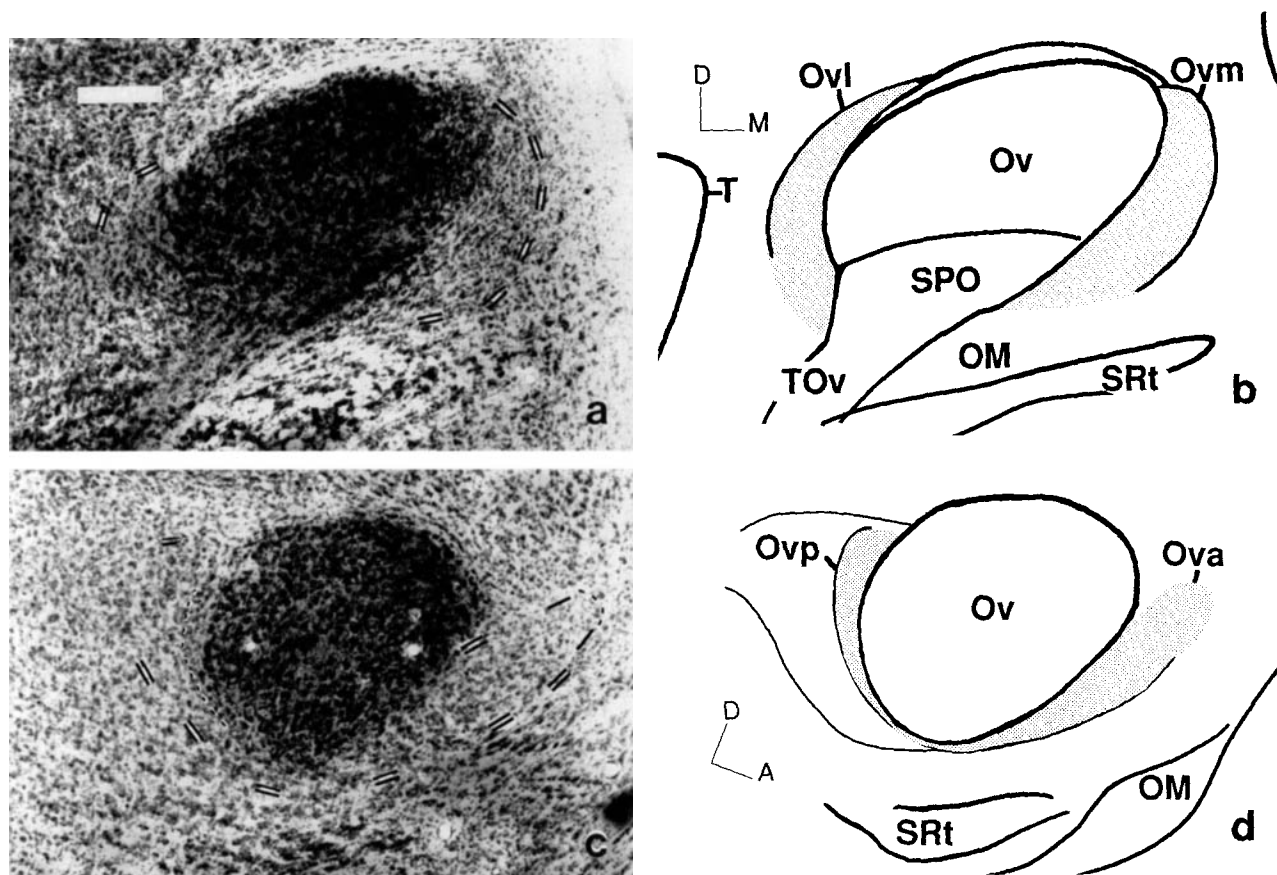
Fig. 1. Matched photomicrographs and drawings of Ov and surrounding cell groups, as viewed with Nissl-staining, in coronal (a and b) and parasagittal (c and d) sections. Scale bar, 200 μm.

ous activity was measured for 1 minute prior to and, in most cases, for 1 minute after testing the response of the unit to the stimulus set, which consisted of 500 ms white noise bursts at 1/second, pure tones and recorded vocalizations. Only the responses to white noise stimulation will be presented here.

Following recording sessions, the last recording site was marked by iontophoresis of PSB dye by passing 10 μA negative current for 20 minutes through the recording electrode. Birds were then given a lethal i.m. injection of chloropent and intracardially perfused with 10% formalin. Brains were frozen, sectioned at 100 μm and counterstained with neutral red.

Nomenclature

Three atlases were used as references. The nomenclature used in this paper is largely based on that of the Karten and Hodos ('67) atlas for the pigeon, with the exception of hypothalamic nomenclature, which follows that of the Kuenzel and Masson ('88) atlas for the chick. The coordinates (in mm) presented in the text and figure legends of the Results refer to brain levels in the Karten and Hodos ('67) atlas and do not represent actual locations in the dove brain (which is slightly smaller than that of the pigeon and requires the following correction factors applied to the atlas coordinates: AP × 0.66, ML × 0.9, DV × 0.75). The plane of section in the atlas for the ring dove by Vowles et al. ('75) corresponded to the head angle, relative to the interaural

line, of the subjects of anterograde tracing experiments from the thalamus, retrograde tracing and electrophysiological experiments. This atlas was therefore useful as an initial guide for the selection of stereotaxic coordinates.

RESULTS
Definition of the Ov shell

The nucleus ovoidalis (Ov) of the ring dove lies in the medial portion of the dorsal thalamus, approximately 350 μm from the midline. It extends roughly 700 μm mediolaterally and dorsoventrally and about 600 μm in the anteroposterior plane. In Nissl-stained sections, Ov can be distinguished as a region of densely packed medium-sized neurons that are larger, rounder, and more darkly stained than immediately adjacent tissue. The nucleus ovoidalis was contiguous with a ventral region, from which it could be distinguished by a slight discontinuity in cell density and alignment. Neurons within this ventral region were similar in size, morphology, and staining characteristics to Ov neurons, but tended to be aligned with their long axes parallel to incoming fascicles of TOv. This region was identified as the nucleus semilunaris parovoidalis (SPO), which extended into TOv along its ventrolateral margin (Fig. 1). In Nissl-stained tissue, measurements of the long axis of 98 cells from central regions of Ov yielded an average of 17.4 ± 2.55 μm (mean ± s.d.), close to the average reported by Bell et al. ('89). Neurons in central regions of

Ov were significantly larger than neurons (n = 81) from the outermost layer of the nucleus along its anterior, posterior, and medial aspects (Student's t = 10.33, d.f. = 177, P < .001). Neurons in this outer layer averaged 13.7 ± 2.23 μm and could be distinguished from adjacent cells of the Ov periphery on the basis of their relatively high concentration of Nissl substance, a feature of the Ov-SPO complex.

In coronal section (Fig. 1a,b), two areas immediately lateral and medial to Ov, Ovl, and Ovm, respectively, consisted of oblong neurons that were less densely packed than those composing Ov and were arranged with their long axes parallel to that of the nucleus. The width of these cell groups decreased as they extended towards the dorsal aspect of Ov, where the nucleus is bordered by a fiber capsule. In parasagittal section (Fig. 1c,d), areas that had a similar cytoarchitecture could be seen to extend from anterior and posterior Ov, and were respectively designated Ova and Ovp. The caudal border of Ovp was ill defined. The average maximum dimension of 61 Nissl-stained cells across all portions of the shell was 13.1 ± 2.21 μm, which was not significantly different from the average calculated for cells of the Ov rim.

Neurons that were labeled by injections of PHAL into peripheral portions of the Ov-SPO complex shared a common morphology. Figure 2 contains camera lucida drawings of representative PHAL-labeled neurons from an injection into Ova. These cells demonstrated features also observed in PHAL-labeled neurons in Ovp, Ovl, and Ovm. Most of the neurons were aligned with their long axes and a set of primary dendrites parallel to the Ov border. Other dendrites appeared to run orthogonally to these, across the plane of section. No dendrites were observed to penetrate into Ov proper. (PHAL-labeled neurons consistently had maximum dimensions larger than those calculated from Nissl-stained tissue of the same region, suggesting that measurements of Nissl-stained material underestimated actual size.)

Injections of PHAL that filled cells along the interface of ICo and MLd (Fig. 3a,b) labeled a bilateral projection to the thalamus and a projection to the medial rim of the contralateral MLd. The thalamic terminal fields were largely constrained to a region surrounding the Ov-SPO complex (Fig. 3c–f), although several small localized patches of labeled fibers and terminal specializations were visible in some sections through central regions of Ov and its anteromedial pole (Fig. 3c). With the exception of the dorsal and dorsolateral aspects of Ov, labeled axons were densely distributed along the Ov rim and within the region peripheral to Ov that was distinguished from the core of Ov-SPO on the basis of cytoarchitecture in Nissl-stained material. These data implicated this peripheral region as a unique subdivision of the auditory thalamus, which was designated the Ov shell.

Although fibers coursed over the dorsal margin of caudolateral Ov, this did not appear to be a major site of termination. The distribution of labeled axons was exceptionally dense along the caudal rim of Ov; however, as was observed in Nissl-stained material, the caudal border of Ovp was difficult to determine; labeled axons in this portion of the shell formed an end-zone consisting of a loose network of fibers and terminal specializations that gradually decreased in width with increasing distance from Ov (Fig. 3e).

The discrete nature of the pathway from the medial margin of MLd to the shell of the auditory thalamus was confirmed with biocytin injections placed medial, lateral, rostral, and ventral to the region that contained well-
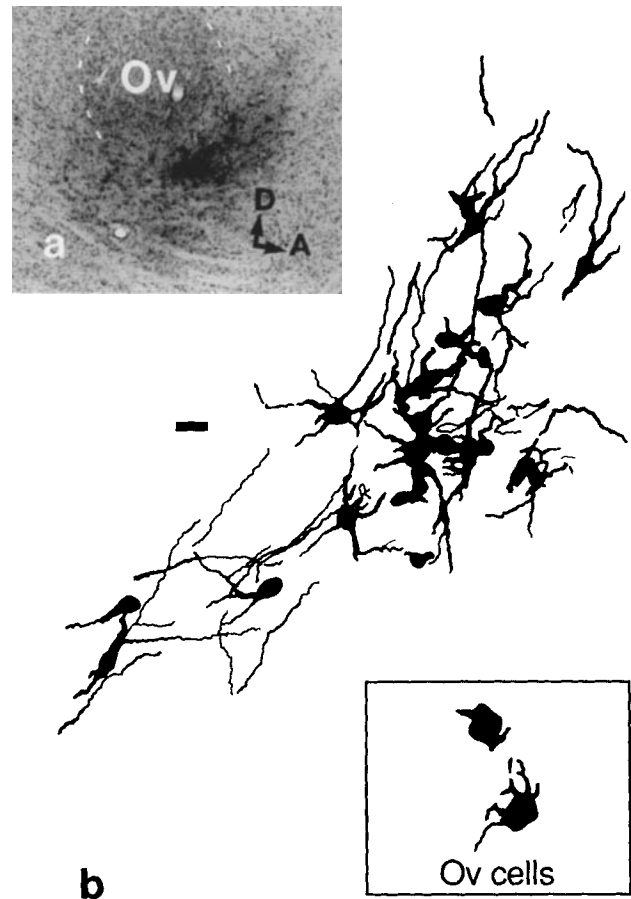

Fig. 2. The injection site in Ova, viewed in lightly counterstained parasagittal section (a), contained well-defined, filled neurons that were drawn with a camera lucida at high magnification (b, scale bar, 20 μm). For comparison, the inset provides a camera lucida tracing of two weakly labeled "ghost" neurons (Gerfen and Sawchenko, '84) from Ov that were labeled from an injection into Ovl. The light labeling of these Ov cells permitted only limited visualization of dendrites. (Neurons labeled from injections into Ov were too densely packed for camera lucida drawing.)

labeled neurons following injections of PHAL. The relative location of medial and lateral injection sites, injections into MLd and ICo, respectively, are identified in Figure 3b. An injection of biocytin into the anterior ICo was analyzed in parasagittal section, as was an injection placed within the ventral margin of medial MLd (not shown). The injection into medial MLd (Fig. 3b) was located approx. 150 μm from the medial rim of the nucleus and labeled axons within the rostromedial pole of Ov, but not axons within the Ov shell. The injections into the medial (Fig. 3b) and anterior ICo also failed to label axons within the Ov shell but did label axons within cell groups previously identified as ICo targets (Akesson et al., '87). The injection into the ventral marginal zone of medial MLd gave rise to labeled fibers within central, dorsal, and caudal portions of Ov, but labeled only an occasional axon in the Ov shell.

Acoustically responsive units were identified within both the shell and its end-zone. Recording sites for these units are presented in Figure 4a: 8 single unit recordings were made rostral to Ov and 13 caudal to the nucleus. Multi-unit activity was recorded along the anterior and medial Ov rim
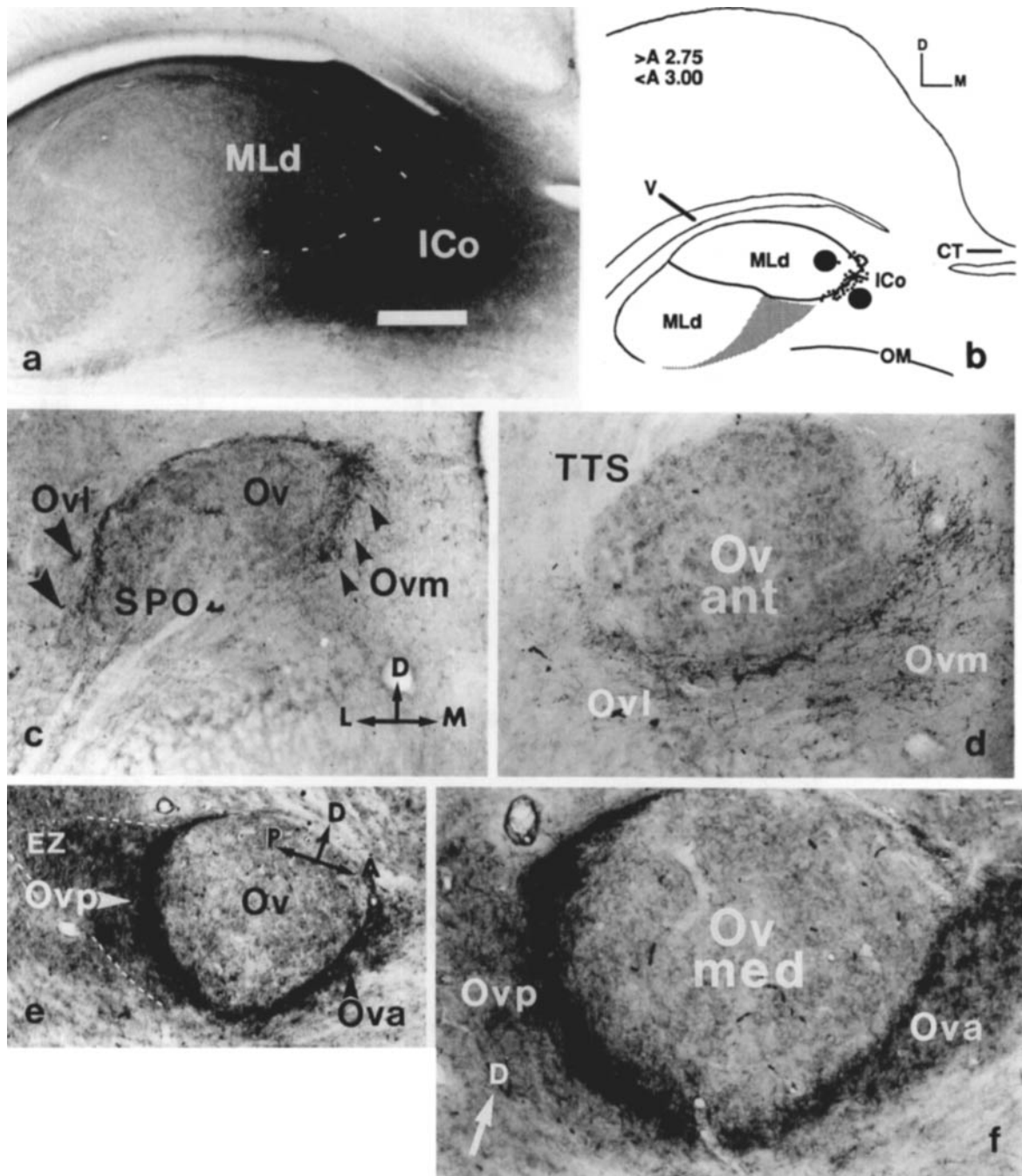
Fig. 3. PHAL injections into the interface region of medial MLd and ICo labeled a projection to the Ov periphery. **a**: Filled neurons within the PHAL injection site depicted here were distributed along the medial rim of MLd (to left of dotted line). **b**: A composite drawing of camera lucida reconstructions of this injection site (coordinates after Karten and Hodos, '67) illustrates the location of PHAL-filled neurons (small black circles). The relative location of two biocytin injections that did not label the Ov surround are superimposed on the drawing as large black circles. **c** and **d**: Axons labeled from the injection site shown in **a** were densely distributed within the medial (Ovm) and ventrolateral (Ovl) periphery of the Ov-SPO complex. **e** and **f**: Labeled axons, here from a PHAL injection into the MLd-ICo interface zone viewed in parasagittal section, were also densely distributed within anterior (Ova) and posterior (Ovp) portions of the Ov surround. A region of diffuse innervation, designated the end-zone (EZ), can be seen to extend from caudal Ov. Scale bar, 250 μm in a, c, and e and 100 μm in d and f. (PHAL injections in this figure were performed by MingXue Zuo.)

and within proximal TOv. Three recording sites (delineated by the rectangle in Fig. 4a) fell outside the region observed to contain PHAL-labeled fibers from the midbrain; otherwise, the distribution of single unit and multi-unit recording sites within the Ov surround overlapped the distribution of ascending labeled terminals from the midbrain. Responsive units were discovered within a region that extended much further along a caudal trajectory from Ov
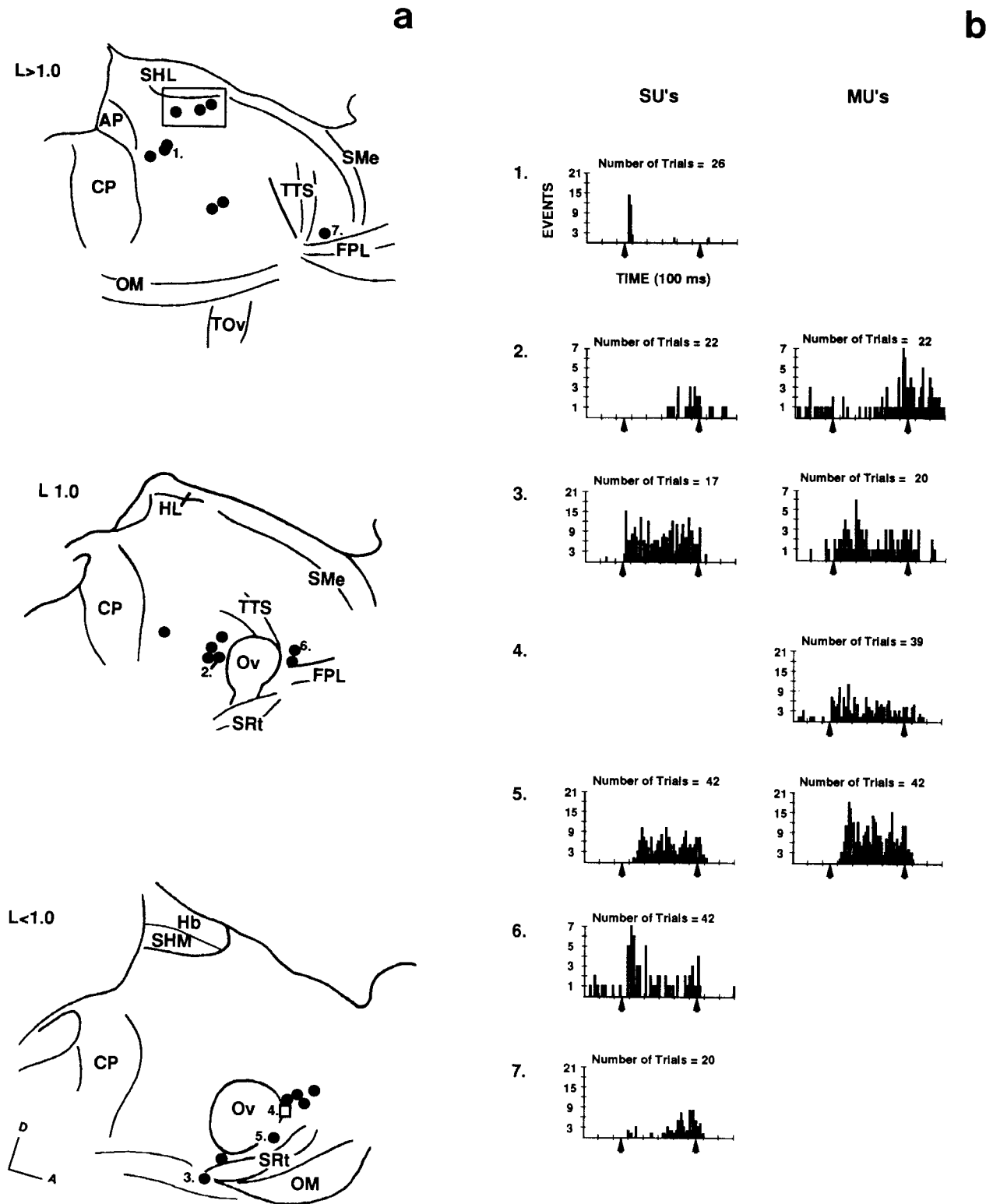
Fig. 4. Camera lucida reconstructions of 100 μm sections containing PSB deposits (recording sites) are depicted as three composite schematics in **a**. Parasagittal coordinates are approximations based upon the Karten and Hodos atlas ('67). Recording sites are presented as black circles (single unit or single unit and multi-unit) and an open square (a multi-unit only site). Sites distributed outside the shell and its end-zone are boxed. Numbers 1–7 designate sites for which responses to 500 ms noise bursts are displayed as peri-stimulus time histograms (**b**). SU, single unit; MU, multi-unit. Arrows denote stimulus onset and offset. Bin size for all PSTHs was 10 ms. A variety of responses are depicted: onset (PSTH 1), inhibitory (PSTH 2), bursting (PSTH 5), decremental (PSTH 4 and 6) and incremental (PSTH 7). Simple tonic-on responses (PSTH 3) were uncommon. (Su and MU PSTHs in 3 were recorded from separate sites.)

than rostral to the nucleus, as was true for labeled fibers ascending from the medial margin of MLd.

Examples of activity elicited by white noise are presented as peri-stimulus time histograms (PSTHs). With the exception of one unit within Ova that had a firing rate of 8.0 ± 0.25 spikes/second (Fig. 4b, PSTH 6), acoustically responsive single units exhibited very low levels of activity in the absence of auditory stimuli (<1 spike/second), values comparable to what has been reported for such units in the dorsal thalamus of the pigeon (Korzeniewska and Güntürkün, '90). Responses to noise bursts were variable and complex (see Fig. 4b).

Ov efferent pathways

The distribution of terminal labeling from four PHAL injections into Ov provided a basis of comparison for mapping efferent pathways labeled from the Ov shell. Two small injections were confined to, respectively, the laterodorsal and mediodorsal portions of rostral Ov. The former case, sectioned coronally, resulted in label within a localized region of ventral L_2. In the latter case, sectioned parasagittally, the diffusion zone extended into the dorsal Ova. Labeled axons resembled those of the case illustrated in Figure 5 but did not extend into as far into the dorsal auditory neostriatum or enter caudally adjacent regions. A third injection completely filled Ov but resulted in relatively light axonal labeling and diffusion of the tracer into Ovp. Lightly labeled fibers were found within all the areas identified in Figure 5 as recipients of Ov axons. In the case illustrated here, some diffusion of the tracer occurred along the track of the micropipette (Fig. 5a) but was negligible within the Ov shell. Caudal and lateral Ov were largely spared by this injection. This case was also characterized by a small arborization of relatively lightly labeled axons within central portions of contralateral Ov. We believe this result to be artifactual and possibly associated with retrograde transport of the tracer (see Discussion).

Terminal fields and trajectories of axons labeled from Ov are depicted in Figure 5b. Ascending axons traveled rostrolaterally from the nucleus within the lateral forebrain bundle and turned caudally upon entering the ventral paleostriatum. Non-branching, non-varicose axons rose into the paleostriatum augmentatum (PA), where they turned caudally towards the lamina medullaris dorsalis. Prior to penetrating this lamina, a small group of weakly branching varicose fibers broke from the fiber group and descended into the ventral PA. Axons invaded the neostriatum primarily via a dorsomedial trajectory, following the course of the capsula interna occipitalis. As anticipated, the distribution of the major terminal field of this fiber bundle within the neostriatum caudale (NC) corresponded to a dense crescent-shaped grouping of small oblong neurons, more uniform in size and arrangement than surrounding tissue. This cell group corresponded to Karten's ('68) description of the pigeon field L, subsequently renamed field L_2 (Bonke et al., '79a). Terminal labeling was observed within L_2 from a parasagittal level of ML 0.5 to a level of ML 2.5. The region of maximum fiber density occurred within the central portion of this field (Fig. 5c) and corresponded to field L_{2a} (Wild et al., '90). Negligible label was observed within the ventromedial end-zone of L_{2a} at the level of the anterior commissure, hereafter referred to as L_2v. The dorsolateral end-zone of L_2, L_{2b} also received few labeled fibers.

Auditory regions bordering L_2, zones L_1 and L_3 (Bonke et al., '79a,b), received a small number of labeled axons. Some

axons arborized immediately upon crossing the lamina medullaris, placing them ventrolateral to L_2 and within field L_3. No arborizations were observed within L_1, a wedge of tissue 300–500 μm wide between L_2 and the lamina hyperstriatica, identified in parasagittal sections as a cell sparse band bordering rostral NC. However, widely scattered varicose axons exited the rostromedial margin of L_2 along a dorsal trajectory, traversed L_1, and penetrated the lamina hyperstriatica into the ventral hyperstriatum (HV). These fibers extended only a short distance into the hyperstriatum (Fig. 5d). Another small group of fibers extended caudally and dorsally from L_2 (same figure) into a region that was identified as the neostriatum dorsale (Nd), after Bonke et al. ('79a). Sparsely distributed fibers within Nd extended to 100 μm of the caudal rim of NC. These axons were sparsely branched but exhibited large varicosities (≥ 2 μm) commensurate in size to large varicosities within L_2 and HV.

Efferent pathways of the anterior and posterior shell

Single injections into the anterior and into the posterior Ov shell were each viewed in the parasagittal plane, enabling these portions of the shell to be viewed together with Ov in the same section. Composite plots of the location of filled neurons within each injection site (Fig. 6a,b) illustrate that labeled terminals in these cases originated from the Ov shell. Telencephalic projections of Ova and Ovp targeted peripheral zones of field L (L_1 and L_3) as well as regions lateral and medial to these zones. A *diencephalic* projection terminated within the hypothalamus in both cases.

The major trajectory of the thalamotelencephalic pathway from Ova and Ovp followed a ventrolateral route through the paleostriatal complex, collateralizing extensively within the ventral paleostriatum (Kitt and Brauth, '81) and ventral PA. Axons in this fiber bundle entered the neostriatum caudolateral to the path followed by Ov axons and rose within the neostriatum caudale along a trajectory that ran parallel to its caudal rim as a sparsely arborizing column of fibers that innervated a wide swath of tissue (Fig. 7a). This terminal field, designated the neostriatum caudale, pars lateralis (NCl), reached its maximum extent approximately 2.0 mm lateral to L_2.

Within the paleostriatum, axons broke from the fiber bundle innervating NCl and ascended into the neostriatum medial to the NCl terminal field. Some axons from Ovp neurons within this side branch rose through L_3 and terminated as a field of highly arborized fibers beneath the lateral edge of ventral hyperstriatum, subadjacent to the lamina hyperstriatica (Fig. 7b). This field extended laterally from a parasagittal level of approximately ML 3.0 to ML 3.5 and was tentatively identified as L_2b, since it appeared to form a lateral continuation of the field labeled from Ov proper, which was of negligible extent at these levels (refer to Fig. 5b). A small number of fibers extended from L_2b into the adjacent hyperstriatum and into Nd.

Axons from Ova also passed into L_3, but they continued into Nd and formed a small field along the dorsocaudal rim of the neostriatum at roughly the same parasagittal level as L_2b (Fig. 7c). Some varicose Ova fibers were also observed coursing through L_2 into Nd, but no arborizations were observed within L_2. Another population of axons traversed L_2 and rose into L_1 and the adjacent hyperstriatum. Both cell groups contained localized patches of moderately arborizing fibers (not shown). From the ventral hyperstria-
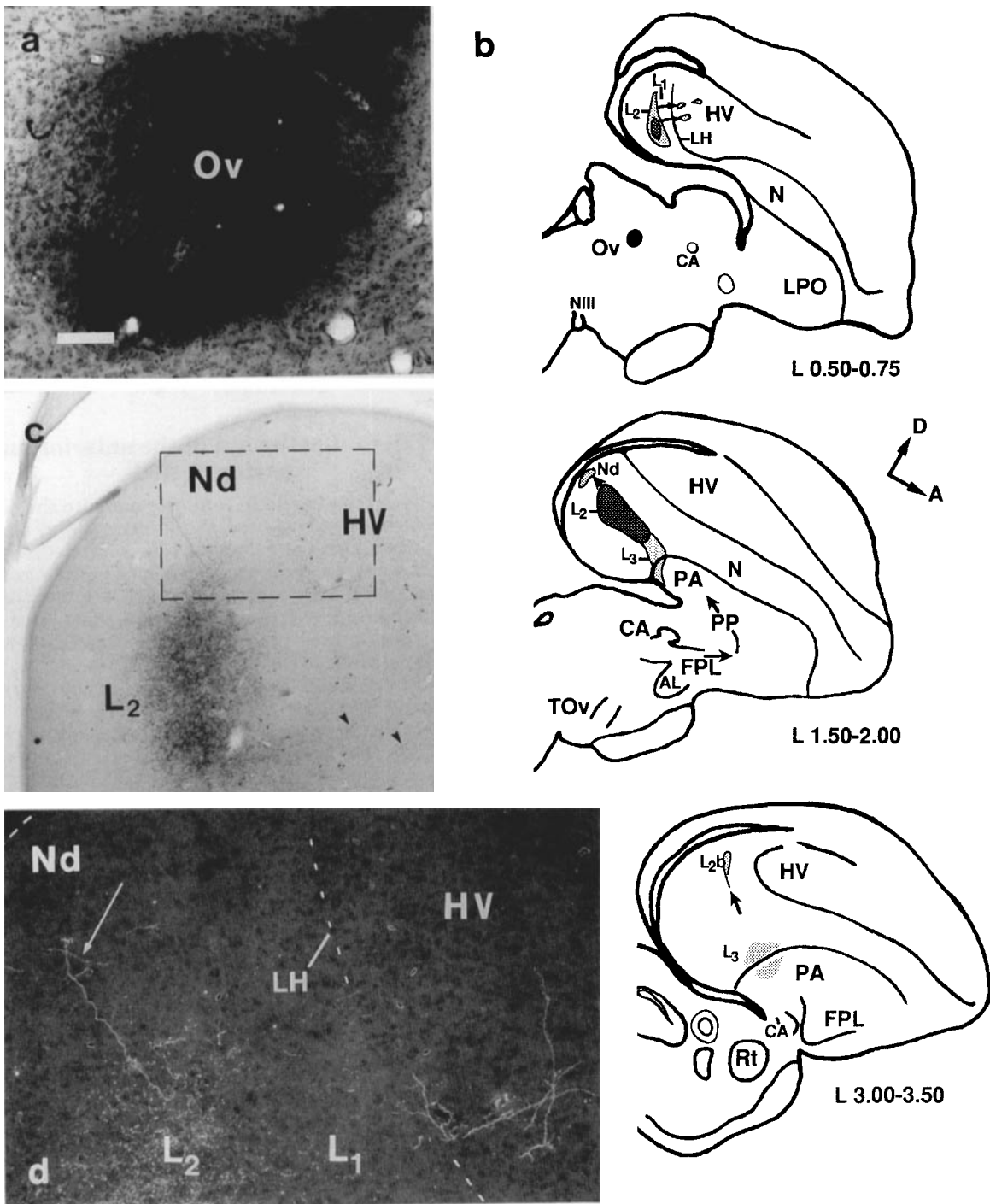
Fig. 5. An injection of PHAL into Ov proper (a) labeled a projection that is depicted schematically in b (parasagittal coordinates after Karten and Hodos, '67). Dark stipling represents areas of dense terminal labeling, such as that *below* the boxed area in c, at a parasagittal level of ML 1.00. Light stipling indicates a light distribu- tion of varicose fibers, as illustrated for HV and Nd in d: Figure d corresponds to the boxed area in c, as viewed in darkfield illumination. Arrowheads in c point to fibers traversing L_1 into HV. Scale bar, 100 μm in a and d and 250 μm in c.

tum, fibers entered the lamina frontalis superior and traveled rostrolaterally within the dorsal telencephalon.

In both these cases, as axons traveled into the paleostria- tum, some fibers appeared to turn back along a ventrome- dial trajectory. This group was thought to be the source of fibers that climbed the periventricular zone of the ventral hyperstriatum and neostriatum caudale, pars medialis (NCm). Axons in these regions were widely dispersed, with large varicosities along their main axis and few side branches (Fig. 7d). Some axons within the hyperstriatal periventricu-
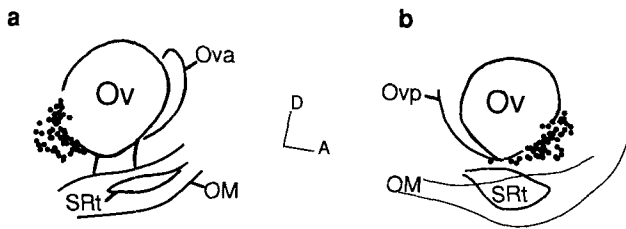
Fig. 6. Composite schematics (dots represent filled neurons) generated from camera lucida reconstructions of PHAL injection sites into Ovp (a) and into Ova (b).

lar zone continued along a dorsal trajectory. Once these axons reached the dorsal margin of the hyperstriatum, they traveled caudolaterally into Nd. Others joined fibers coursing in the lamina frontalis, a group tentatively identified as the source of innervation of the lateral rim of the neostriatum (Fig. 7e).

A number of regions shown to concentrate estrogen by Martinez-Vargas et al. ('76) received projections from Ova and Ovp; these included the dorsal and ventromedial hypothalamus, the periventricular region of the tectum, the septum, and ventral portions of the telencephalon. Most of these projections are illustrated in Figures 8 and 9. As fibers traveled rostrolaterally from Ov within the lateral forebrain bundle, axons split off from this bundle caudal to the anterior commissure and descended into the hypothala-
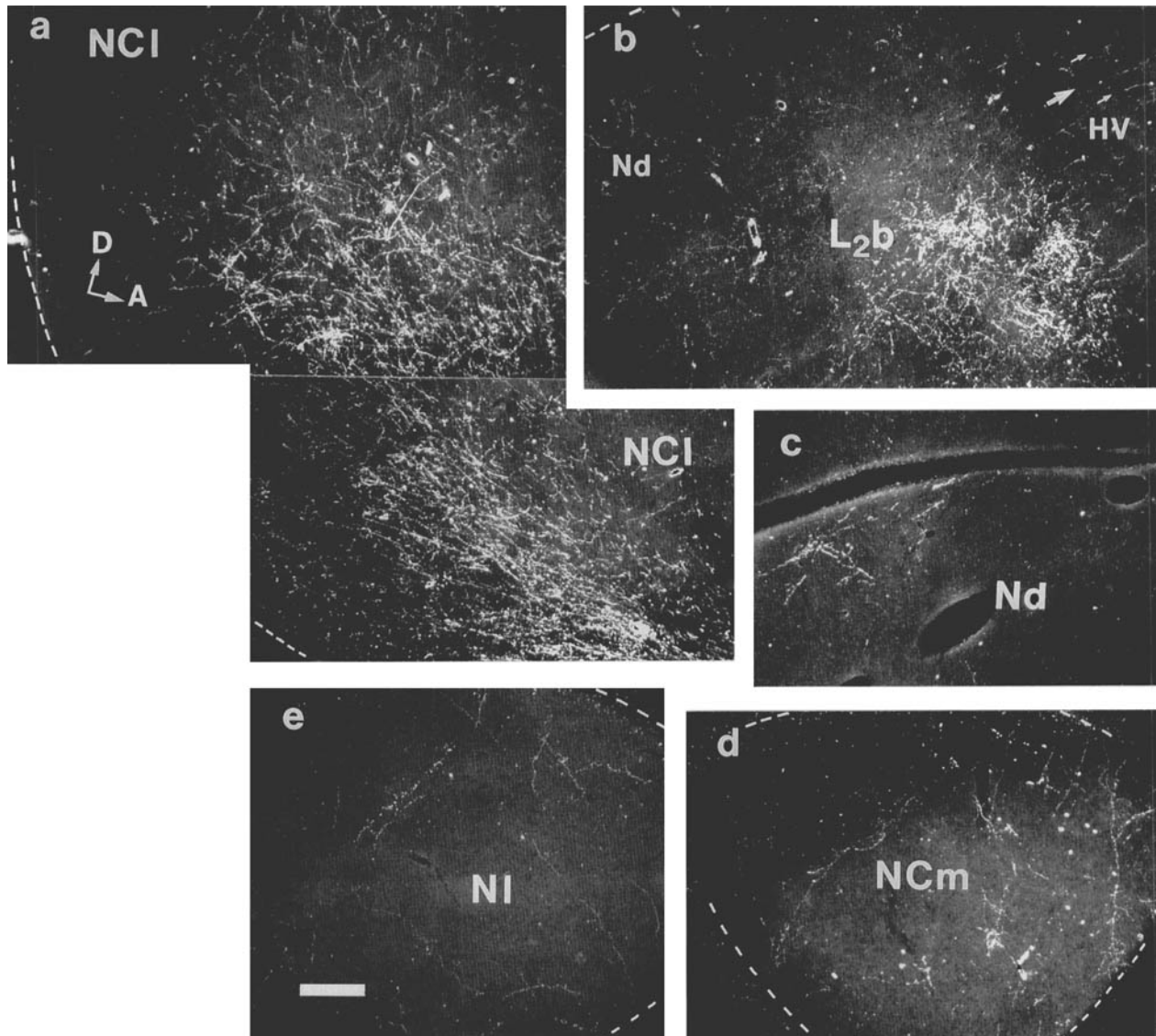
Fig. 7. Neostriatal projections labeled from Ova and Ovp as seen in darkfield illumination: a: (Parasagittal level = ML 4.50). The major telencephalic projection of Ova and Ovp was to NCl. The Ovp projection shown here was particularly robust. b: (ML 3.00) Only Ovp axons terminated in L_2b. A few fibers can be seen extending into HV (arrows) and Nd. c: (ML 3.50) Ova axons formed a small terminal field in Nd. The medial d (ML 0.30) and lateral e (ML 9.00) aspects of the neostriatum received comparable projections from both regions of the shell (d from Ova, e from Ovp). Dotted lines delineate boundaries of the neostriatum. Scale bar, 250 μm.
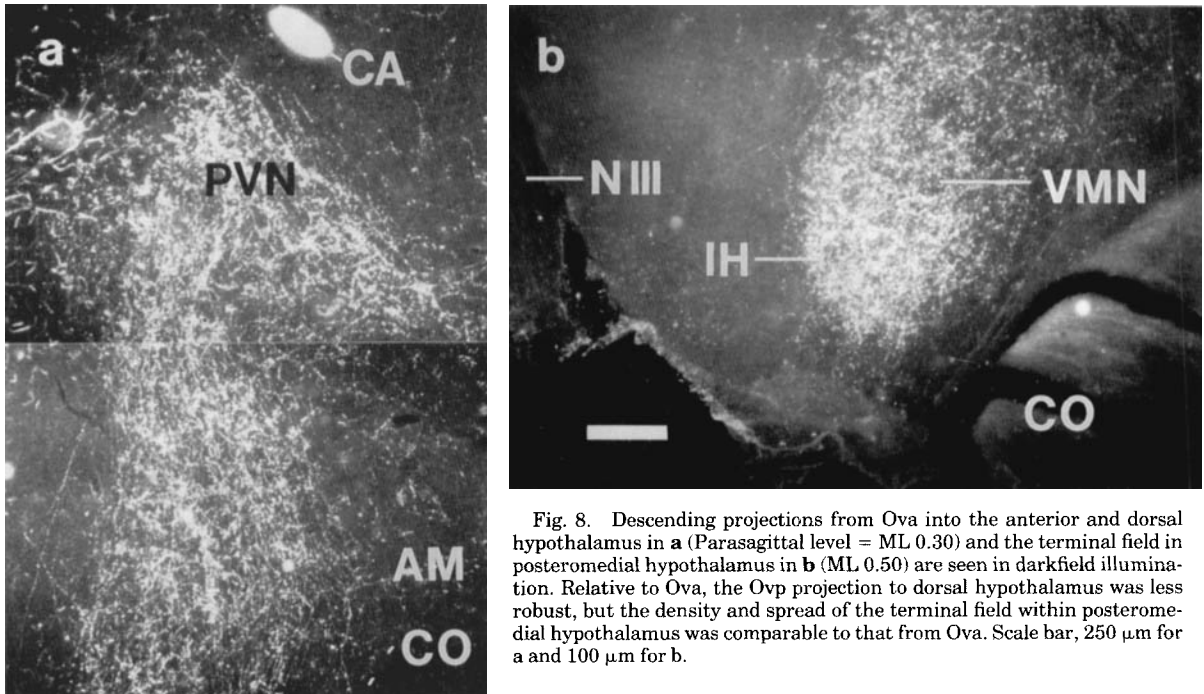
Fig. 8. Descending projections from Ova into the anterior and dorsal hypothalamus in **a** (Parasagittal level = ML 0.30) and the terminal field in posteromedial hypothalamus in **b** (ML 0.50) are seen in darkfield illumination. Relative to Ova, the Ovp projection to dorsal hypothalamus was less robust, but the density and spread of the terminal field within posteromedial hypothalamus was comparable to that from Ova. Scale bar, 250 μm for a and 100 μm for b.
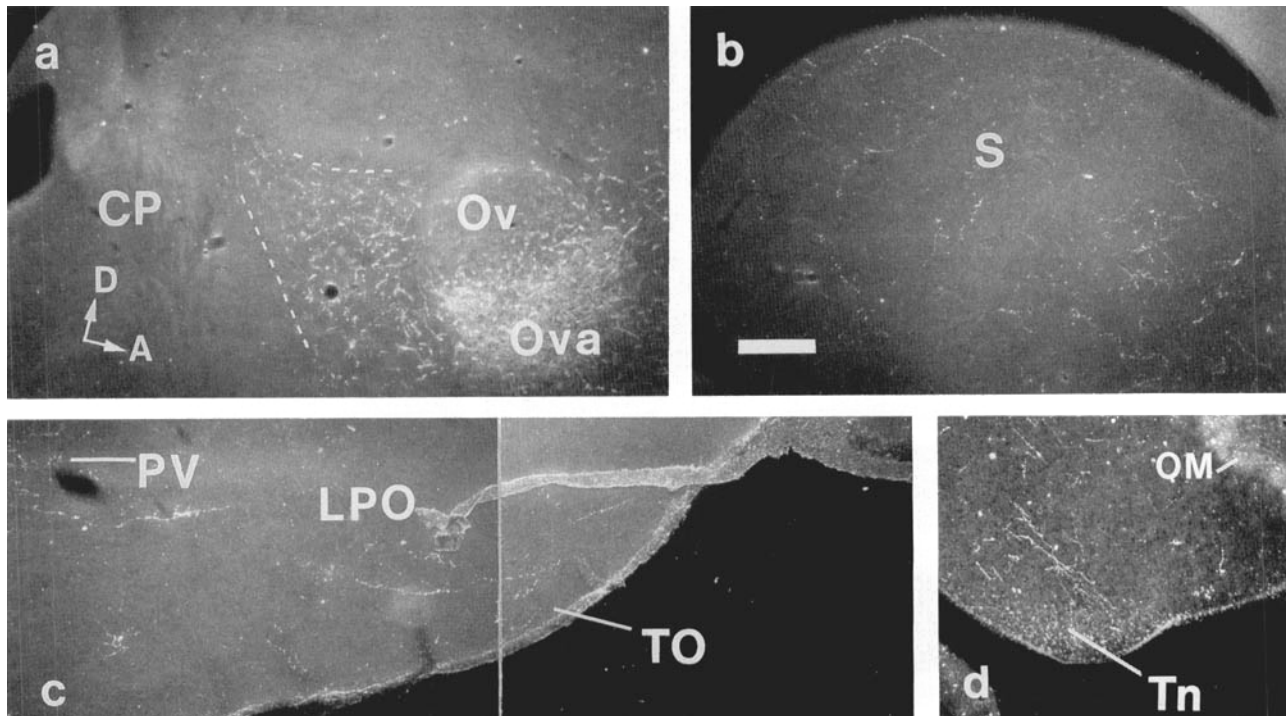

Fig. 9. Darkfield photomicrographs of the dorsal thalamus (**a**), septum (**b**) LPO/TO region (**c**), and Tn (**d**), cell groups that received labeled axons from both Ova and Ovp. a, b, and c were labeled from Ova and d from Ovp. Note (in a) that a region of en passant innervation

within the dorsal thalamus, along a putative pathway from the Ov shell to the midbrain (see text), maps onto the end-zone of the Ov shell. Note (in c) the anterior edge of a labeled field in PV is visible upper left. Scale bar, 250 μm.

mus. The dorsomedial hypothalamus appeared to receive a dense en passant innervation, especially from Ova (Fig. 8a). Most of these descending axons followed a caudomedial trajectory through the dorsal hypothalamus and formed a

dense terminal field within the nucleus inferiori hypothalami (IH) and the caudal nucleus ventromedialis hypothalami (VMN) (Fig. 8b). A smaller number descended from the lateral forebrain bundle directly into the lateral hypothala-

mus and then traveled medially into IH. A few fibers descended into the anterior hypothalamus (Fig. 8a) or descended directly from the medial aspect of Ov into IH.

Several minor projections were labeled from injections into both Ova and Ovp. A small population of varicose axons traveled from Ov along a *caudal* trajectory through the dorsal hypothalamus (Fig. 9a). It was not clear whether these fibers entered the tectal or posterior commissure or both, but they were judged as the most likely source of varicose axonal segments scattered within the periventricular region of the tectal ventricle and, more diffusely, within ICo and the midbrain central grey. Rostral and lateral to where the hypothalamic projection broke from the main fiber bundle, axons ascended medially into the septum (Fig. 9b), while others continued into the more anterior regions of ventromedial parolfactory lobe and olfactory tubercle (Fig. 9c). The nucleus taenia and adjacent archistriatum received a small projection (Fig. 9d) from fibers that broke from the major group of ascending axons as it entered the paleostriatum.

Efferent pathways of the lateral shell

Injections were made into the region lateral to Ov in two birds. These brains were sectioned coronally. An injection into Ovl resulted in diffusion of the tracer throughout the strip of tissue bordered by Ov medially and by the nucleus triangularis laterally (Fig. 10a). Labeled neurons were distributed below the level of the thalamostriatal tract (Fig. 10b), a region previously identified as the lateral portion of the Ov shell (Ovl). An area dorsal to Ovl was also stained by this injection but did not appear to contain filled neurons. However, the intensity of the stain suggested that some axons labeled from the injection into Ovl may have originated from neurons dorsal to Ovl. In order to clarify this issue, the pattern of labeling that resulted from the injection into Ovl was compared with that resulting from a second injection, which was confined to the dorsal portion of the lateral surround of Ov (Ov-dl) and which filled neurons dorsal to the thalamostriatal tract (Fig. 10c,d).

There was little overlap between the two sets of labeled projections. The Ov-dl injection labeled a terminal field in the temporo-parieto-occipital area and a second projection, consisting of more lightly labeled axons, within a portion of the neostriatum medially adjacent to the ectostriatum. Labeled axons were conspicuously absent from all zones of the auditory neostriatum and immediately adjacent regions of the caudal telencephalon. No major diencephalic projection was labeled from Ov-dl, although a few sparsely distributed varicose fibers were present within the lateral hypothalamus. In contrast, the injection that labeled cells in Ovl labeled zones L_1–L_3, HV, Nd, NCl, and the caudomedial hypothalamus. The projection fields of this case are mapped in Figures 11–13.

Both injections labeled minor projections to the lateral rim of the neostriatum, nucleus taenia, olfactory tubercle, ventral paleostriatum, and ventral PA, although Ov-dl fibers were distributed more laterally within this region. The general dissimilarity between the results with respect to the major projections labeled from each site suggested that neurons within Ovl were the source of labeled axons within the auditory neostriatum and surrounding regions, and were also the source of labeled descending pathways. The shared minor targets, primarily consisting of estrogen concentrating regions, were shown to be labeled from other portions of the shell not adjacent to Ov-dl (see parts II and IV of Results). Only pathways labeled from the Ovl injection are described further.

All sections through Ov contained axons labeled from Ovl. These formed a loose network of varicose fibers within central portions of the nucleus. Non-varicose, large diameter axons coursed medially within the dorsal fiber capsule and along the ventral perimeter of Ov-SPO complex. The latter group entered Ovm and then descended into the hypothalamus. As with other shell injections, labeled dendrites did not penetrate Ov.

The distribution of labeled fibers within the telencephalon corresponded closely to that of Ova and Ovp axons, as can be seen in Figures 11–13, but in this case L_2v also contained a small terminal field (Fig. 12d). Axons arborized after passing through the lamina medullaris at the level of the anterior commissure and formed a small, highly localized field bordered by his lamina laterally and the lamina hyperstriatica medially. Zones L_1 and, to a lesser extent, L_2 appeared to receive collateral innervation by fibers that traversed the auditory neostriatum into caudal regions of the ventral hyperstriatum. Neither L_1 nor L_2 was as densely innervated as L_3 (Fig. 12c,f). The trajectory into the periventricular region of the lateral ventricle clearly followed a path that initially rose through the paleostriatum (augmentatum and primitivum) to reach the lamina medullaris dorsalis. Axons then descended medially within this lamina. Upon reaching the periventricular zone, these fibers climbed the medial wall of the ventral hyperstriatum and neostriatum and extended laterally into Nd, as suggested in the parasagittally sectioned cases of Ova and Ovp. Afferent fibers also reached Nd via L_3 (Fig. 13d).

Descending pathways from Ovl corresponded to those from Ova and Ovp; however, the projection to IH (Fig. 13f) was less robust and did not collateralize within the dorsal thalamus. The small projection into the midbrain proved easier to map in coronal section. Axons that traveled into the dorsal thalamus caudal to Ov were diffusely scattered over the nuclei of the posterior thalamus (Fig. 13b). Axons were observed within both the posterior and tectal commissures. A few within the posterior commissure entered the midbrain central grey. Some lightly labeled fibers were also observed within the reticular formation, but the pathway into this region was not identified. Axons that traveled in the tectal commissure passed into the central white layer of the tectum and entered the periventricular region throughout its dorsoventral extent. Here they were sparsely distributed along the rim of the tectal ventricle, where they gave rise to small terminal arborizations (Fig. 13g).

Efferent pathways of the medial shell

In two birds, injections were made into the medial shell (Fig. 14a). These injections yielded similar distributions of labeled fibers. Fewer than ten neurons could be clearly distinguished at the injection site in each case and their locations are plotted in a composite schematic in Figure 14b. In these cases telencephalic projections were limited to previously identified targets within the medial telencephalon. The lateral component of telencephalic projections from Ova, Ovp, and Ovl was absent. Telencephalic targets included the ventral paleostriatum and ventral PA, endzones of field L, caudomedial regions of the ventral hyperstriatum, and NCm. Zones L_1 and L_3 appeared to receive some en passant innervation from highly varicose fibers
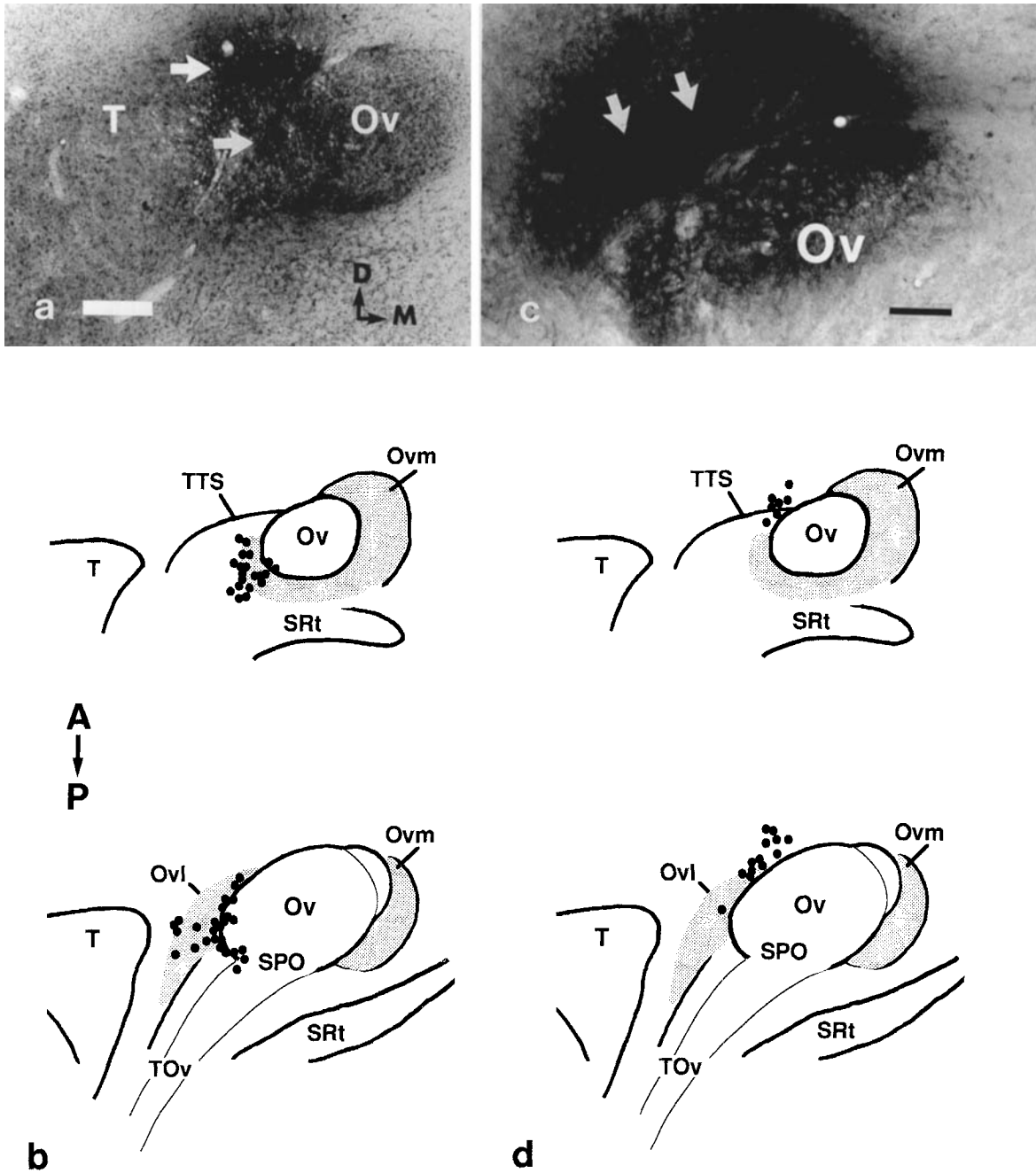
Fig. 10. The distribution of labeled neurons is compared between injections into Ovl and Ov-dl. The Ovl injection site (a) was characterized by a patch of stained tissue (top arrow) dorsal to the region that contained filled neurons (bottom arrow) that are mapped schematically in b. The injection site into Ov-dl (c) corresponded in location to the re-

gion marked by the top arrow in a. Filled neurons from the Ov-dl injection were distributed below the two arrows and above the fiber bundle that forms the dorsal rim of Ov. These cells are mapped in d. Scale bars: a, 250 μm; c, 100 μm.

passing into, respectively, L_{2b} and the hyperstriatum, but negligible arborization occurred within these zones. Axonal trajectories within the medial telencephalon followed pathways established previously and are mapped in Figure 15.

As was the case for Ovl, injections into Ovm labeled a small number of axons, but not dendrites, within Ov. These axons traveled from the injection site along the dorsal rim

of Ov and sparsely arborized within the dorsolateral portion of the nucleus. Axons within the lateral forebrain bundle broke from this tract prior to the anterior commissure and descended into the medial hypothalamus along two trajectories, either along a pathway into the lateral hypothalamus that then turned medially or along a medially directed pathway that then descended into the hypothalamus along
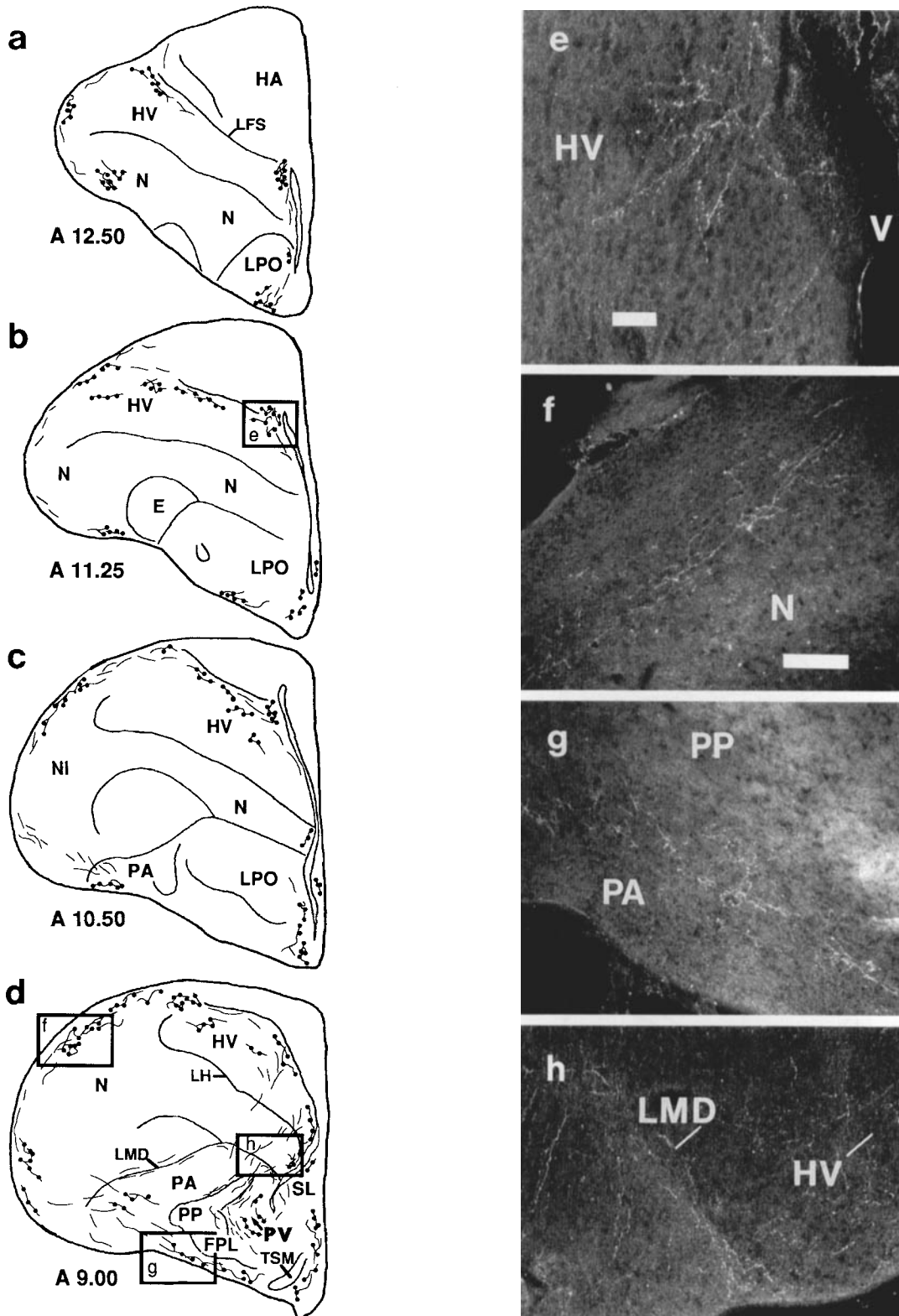
Fig. 11. Projections labeled from Ovl are mapped schematically in consecutive coronal sections that are presented in rostral to caudal series. Coordinates are approximations from Karten and Hodos ('67). Drawings of labeled fibers (not to scale) indicate fiber orientation, the presence or absence of varicosities, and relative density and distribution. Lettered boxed areas on the schematics correspond to photomicrographs of the same letter. Scale bars: e, 100 μm; f–h, 250 μm.
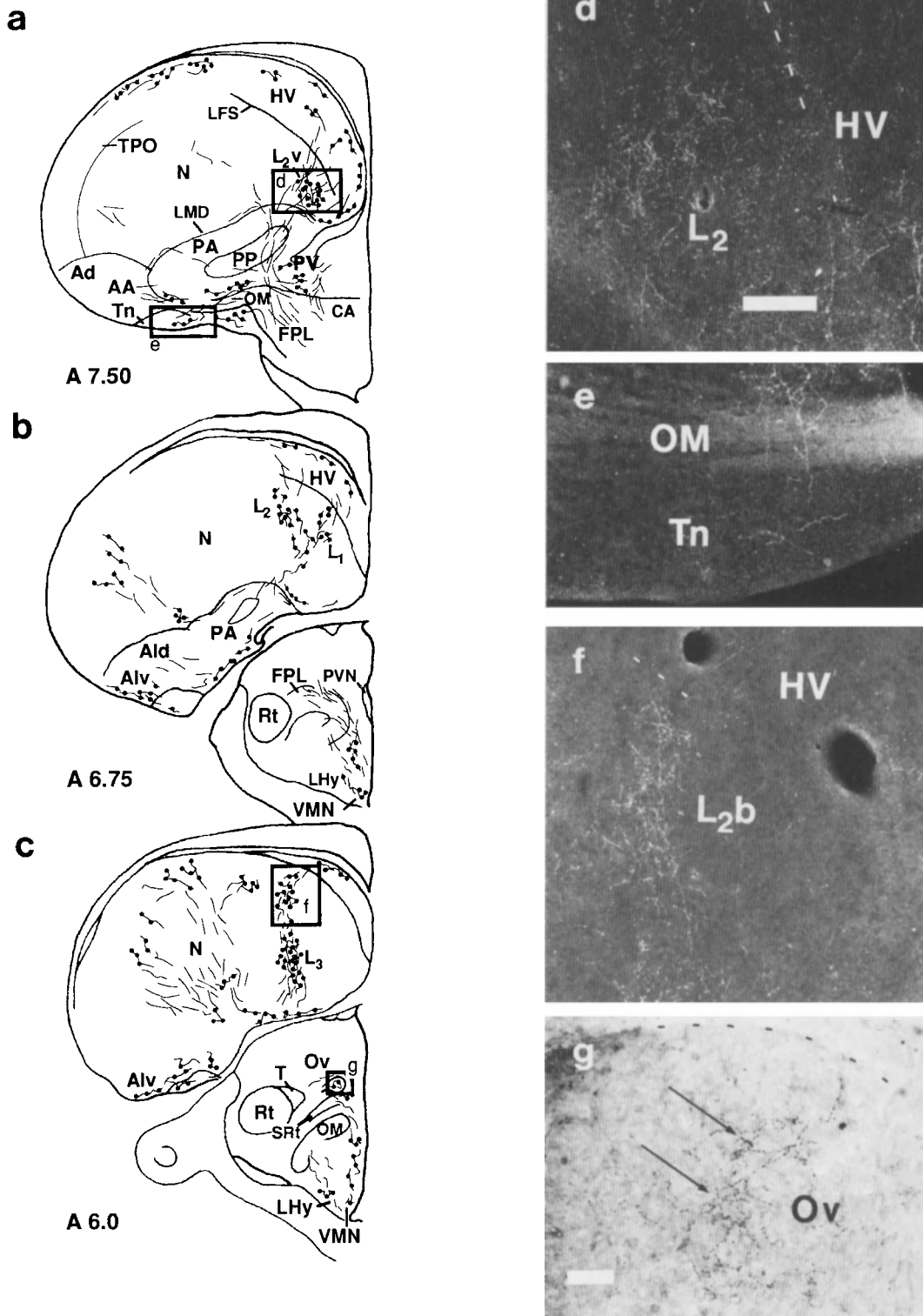
Fig. 12. Caudal continuation (see Fig. 11) of mapped projections labeled from an injection into Ovl.
Arrows in g point to varicose axons in Ov. Scale bars: d–f, 250 μm; g, 100 μm.

the midline. Within the latter pathway, fibers weakly arborized throughout their descent in the dorsal hypothalamus, which appeared as densely innervated as VMN in these cases. There were relatively few fibers within IH and only a few axons could be found within the periventricular grey layer of the tectum.
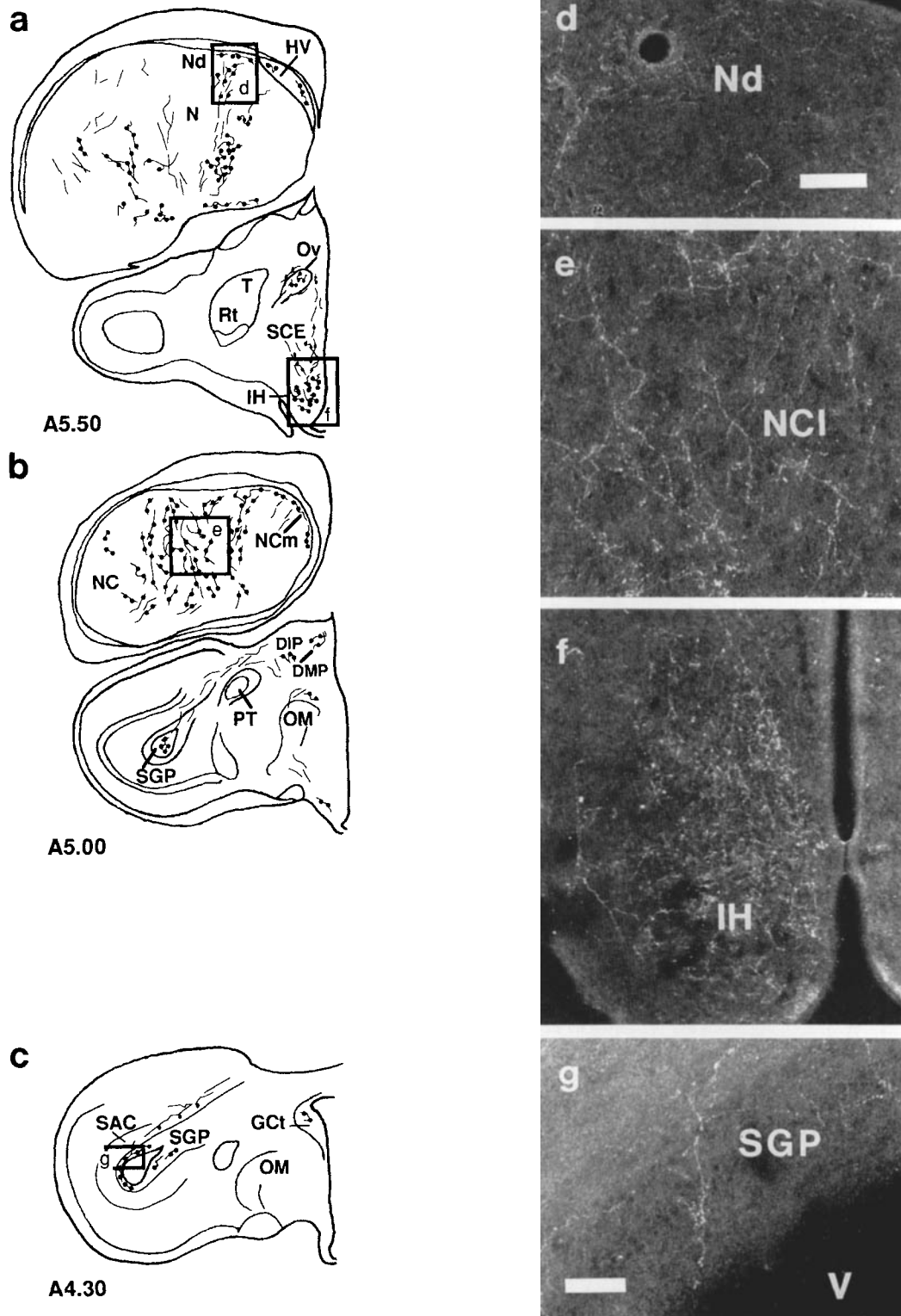
Fig. 13. Caudal continuation (see Figs. 11, 12) of mapped projections labeled from an injection into Ovl. c depicts only the tectum; no labeled axons were found in the telencephalon at this level. Scale bars: d–f, 250 μm; g, 100 μm.
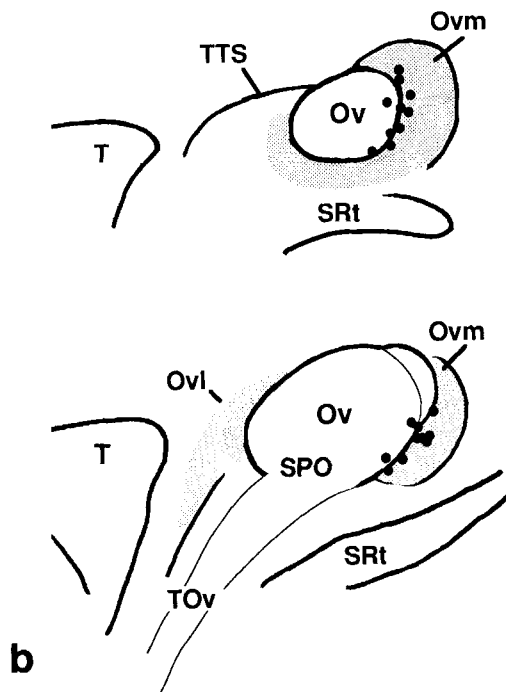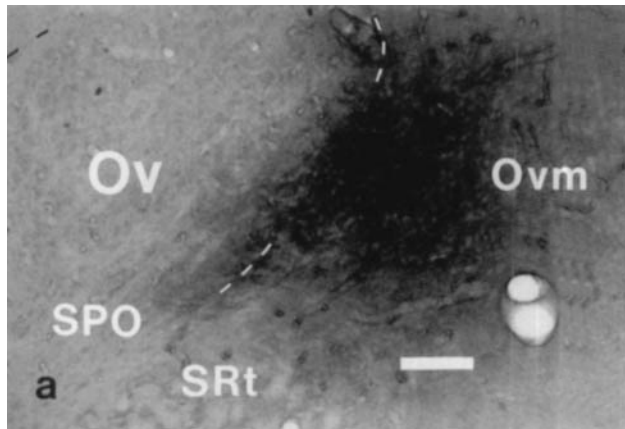
Fig. 14. One of two small injections into Ovm is depicted in **a**. In **b**, labeled neurons (dots) from both injections are presented as a composite schematic. Scale bar in a, 100 μm.

Retrogradely labeled pathways

Hypothalamic injections of fluorogold provided a comparison with the PHAL labeled pathways described above. In all cases, the track of the syringe needle passed rostral to Ov. Two brains that received, respectively, 0.07 μl and 0.15 μl of the tracer were sectioned in the parasagittal plane. The smaller injection was centered within IH, with spread of the tracer into VMN (Fig. 16a). The larger injection was more dorsally situated and the label penetrated the stratum cellulare externum as well as the posterior portion of IH and posterodorsal VMN (Fig. 16b).

Neurons within Ova displayed dense retrograde labeling in these cases, whereas neurons within Ovp were lightly scattered throughout this portion of the shell (Fig. 17a–c). Labeled neurons were absent dorsally. In both parasagittally sectioned cases, sections through medial Ov, which

incorporated ventral portions of Ovm as well as Ova, contained a higher population of labeled neurons. Neurons within Figure 17a,b were filled by the injection into IH (Fig. 16a). A comparison of Figure 17b with 17c, which was labeled by the fluorogold injection that encompassed regions of the dorsal hypothalamus and VMN, reveals a difference in the distribution of retrograde label between the two cases. Neurons comprising the Ov rim are labeled in Figure 17c, but not in 17b, thus suggesting that this cell group may be more closely associated with a projection to the dorsal hypothalamus than are other regions of the shell. This variation in the distribution of label was most apparent in lateral sections.

In a third case that was sectioned coronally, 0.07 μl of the retrograde tracer was injected into caudal VMN and spread into the anterior portion of IH and slightly into SCE. Labeled cells were densely distributed within Ovm (Fig. 18a) throughout the rostrocaudal extent of Ov and were diffusely scattered within the ventrolateral shell and proximal TOv. Other brain regions labeled by these hypothalamic injections included the midbrain central grey and the nucleus preopticus.

The injection of fluorogold into the ventral paleostriatum and ventral PA resulted in labeled neurons within Ov proper and the Ov shell (Fig. 19a). Differences in morphology and size between labeled neurons of the Ov core and shell, discussed in section 1, are readily apparent when retrogradely labeled cells from this injection are compared across the two regions (Fig. 19b,c). Filled neurons were localized to the ventral portion of medial Ov (Fig. 19b) and were scattered throughout Ov in more lateral regions of the nucleus (Fig. 19c). A group of cells in Ovp was labeled throughout the mediolateral extent of the nucleus; however, labeled neurons within Ova were more numerous within the lateral portion of the shell. This injection also labeled Ovl and a few scattered neurons within Ovm (not shown). The injection into the paleostriatum resulted in some diffusion of fluorogold into the septum. An injection of 0.15 μl was made into the septum, which resulted in some spread of the tracer into the immediately adjacent dorsal thalamus. Only a few neurons in any given section through the auditory thalamus were labeled in this case, mostly within the anteromedial portion of the Ov shell, and are not shown here. Two 0.15 μl injections into the anterior parolfactory lobe, which spared its ventral edge and the olfactory tubercle, failed to produce labeling either within Ov or its shell, with the exception of an occasional filled neuron along the posteroventral Ov rim.

DISCUSSION
Summary of results

The afferent and efferent connectivity of a region within the avian auditory thalamus was distinguished from previously established auditory pathways associated with Ov. This region was designated the shell of the nucleus ovoidalis and was visible in Nissl-stained tissue. Ascending afferent fibers to shell regions of the nucleus ovoidalis, Ova, Ovp, Ovm, and Ovl, originated from neurons that composed the medial rim of MLd. These neurons formed an interface between MLd and the nucleus intercollicularis, and corresponded to a portion of the auditory midbrain that receives afferents from the nucleus laminaris (Liebler, '75).

The boundary of Ovp was ill defined; the shell extended away from Ov into the caudal thalamus, forming an end-zone to the level of the posterior commissure. As
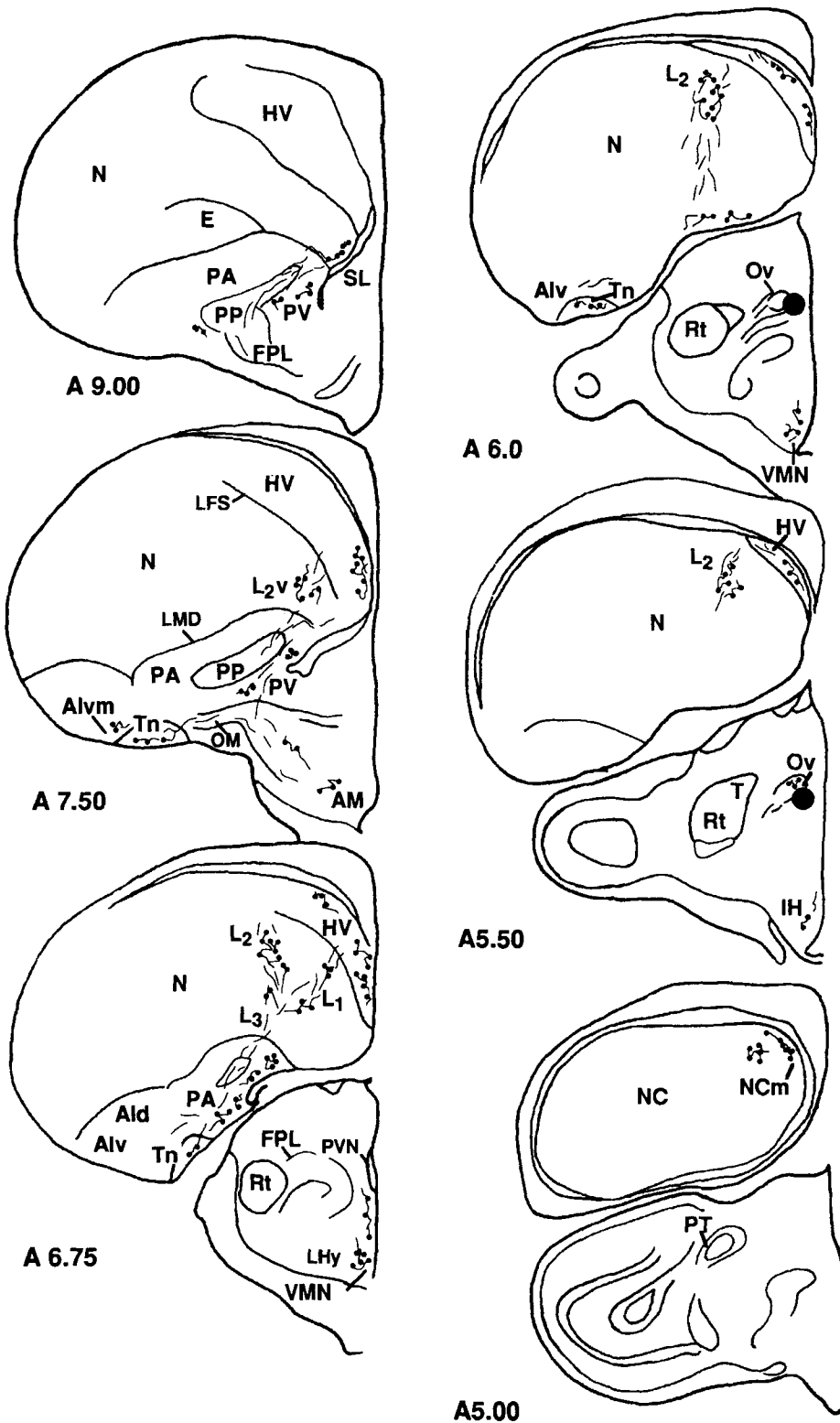
Fig. 15. Projections labeled from Ovm are schematically presented as described for Ovl (see Fig. 11).

characterized by labeled midbrain afferent fibers, this portion of the shell consisted of a diffuse and widely distributed network of axons that overlapped with previously established medial, intermediate, and lateral cell groups within

the posterior dorsal thalamus (DMP, DIP, and DLP). It is possible that recent data (Korzeniewska and Güntürkün, '90) showing auditory evoked responses within the most lateral of these cell groups are attributable to this projec-
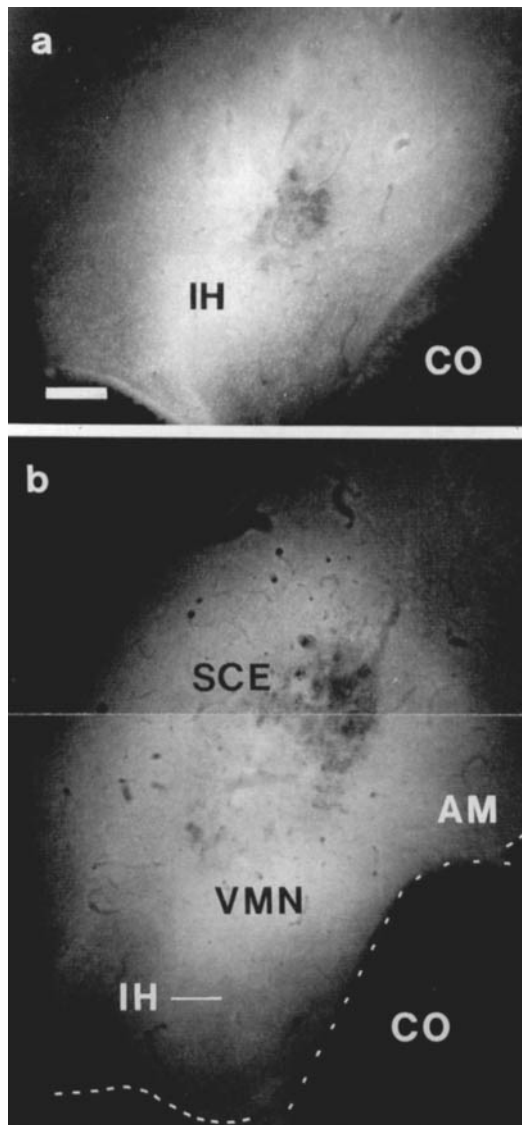
Fig. 16. Two hypothalamic injections of the retrograde tracer fluorogold were situated differently within the hypothalamus, as viewed in parasagittal section. In **a**, the injection is centered within IH, whereas in **b**, which is more dorsally situated, the regions labeled by the injection includes VMN and the ventral portion of SCE. Scale bar, 250 μm.
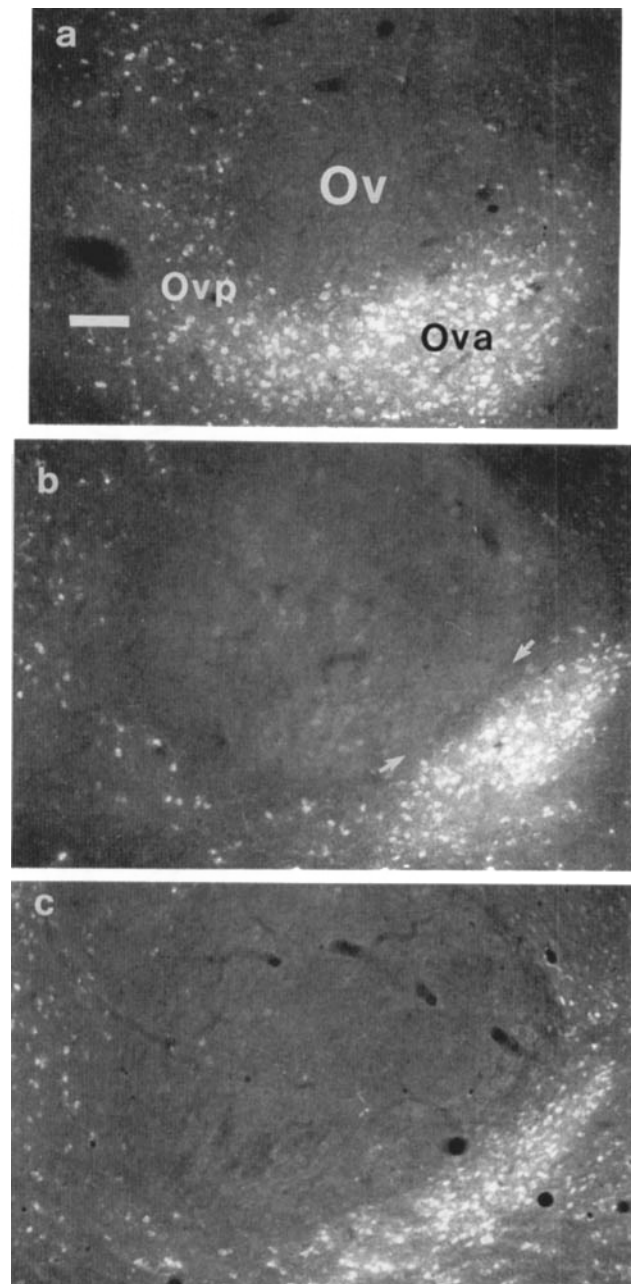

Fig. 17. The sections in **a** and **b** were retrogradely labeled by the injection shown in Figure 16a, whereas **c** was labeled by the injection in Figure 16b. In both cases, a medial to lateral progression through Ov (here illustrated in the progression a to c) was associated with a decrease in the width of the labeled region surrounding Ov. Label was observed in medial Ovp but was negligible in lateral sections. Labeled cells were dispersed within the end-zone of the shell. Arrows in b point to the anterior Ov rim, which appears unlabeled by the IH injection (Fig. 16b), but is labeled (c) from the injection that included the dorsal hypothalamus (Fig. 16a). Scale bar, 100 μm.

tion. In mammals, the inferior colliculus, analogous to MLd, projects to portions of the thalamic posterior complex of nuclei (Kudo and Niimi, '80, LeDoux et al., '85), cell groups that bear similarities to DLP (Korzeniewska and Güntürkün, '90). Acoustically responsive units were found within the shell and its end-zone, as well as dorsal to this terminal field. Some data from our laboratory (Durand et al., unpublished) suggest that units within the latter region may receive afferents from a portion of the shell end-zone.

Pathways labeled with PHAL revealed projections from the auditory thalamus to peripheral zones of the auditory neostriatum (L₁ and L₃) and to components of intratelencephalic auditory pathways: the neostriatum dorsale (Nd), ventral hyperstriatum, paleostriatum, and ventromedial archistriatum, as identified in the chicken and pigeon

(Bonke et al., '79a,b; Wild et al., '90). The medial periventricular zone of the lateral ventricle has also been previously implicated as an auditory area (Brauth, '90, cf. Fig. 1A; Brauth and Reiner, '91, cf. Fig. 6a). A projection to the lateral telencephalon, originating from portions of the shell
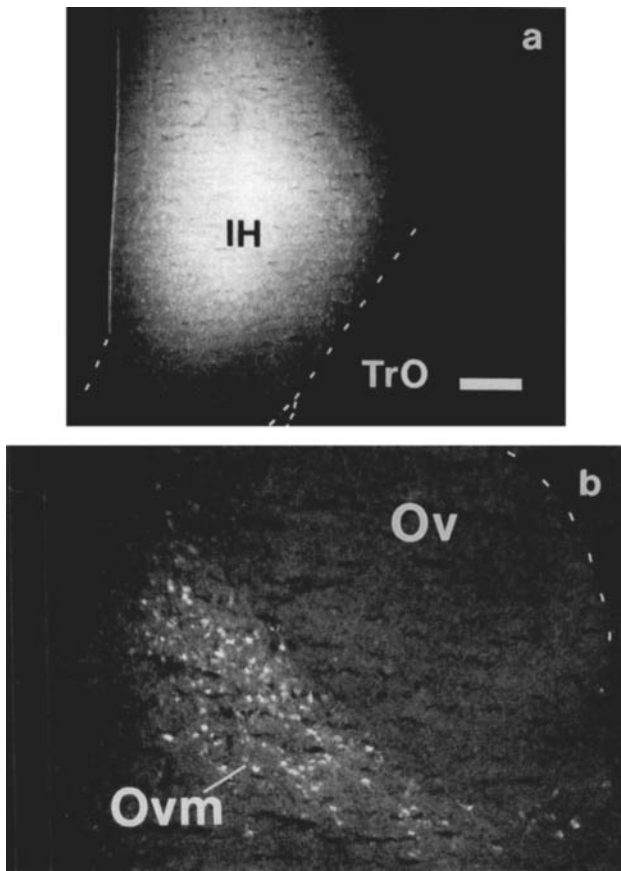
Fig. 18. The fluorogold injection site (a) in this coronally sectioned case encompassed posterior VMN and anterior IH and was of comparable size to the injection shown in Figure 16a. Labeled cells were observed within Ovm (b) throughout the A–P extent of the nucleus. Labeled neurons were also densely distributed rostral and caudal to Ov, but were observed only in the most ventral reaches of Ovl. Scale bar, 250 μm in a and 100 μm in b.

other than Ovm, terminated as a field caudolateral to the auditory neostriatum, NCl.

This study implicates several non-telencephalic nuclei as targets of the Ov shell. Lateral and medial portions of the shell projected onto Ov proper. Two cases of light labelling in the contralateral Ov (from injections into Ov proper and Ovm) are probably artifactual, since retrograde tracing failed to confirm a contralateral projection. It is possible that the labeled axons originated from bilaterally projecting neurons in MLd that were retrogradely labeled from the injection (Wild, personal communication). Some retrograde transport has been demonstrated for PHAL (Shu and Peters, '88).

Pathways from the Ov shell to the hypothalamus were confirmed with retrograde tracing, providing the first evidence for an auditory pathway to the hypothalamus in an avian species. A descending hypothalamic projection was characteristic of all portions of the Ov shell, as were projections to other estrogen concentrating regions (Martinez-Vargas et al., '76). These included the nucleus taenia and a medially adjacent region (Martinez-Vargas et al., '76, cf. Fig. 4D,E) continuous with the ventral paleostriatum (Kitt and Brauth, '81). The tectal periventricular zone, especially its dorsal and lateral portions, received a moder-
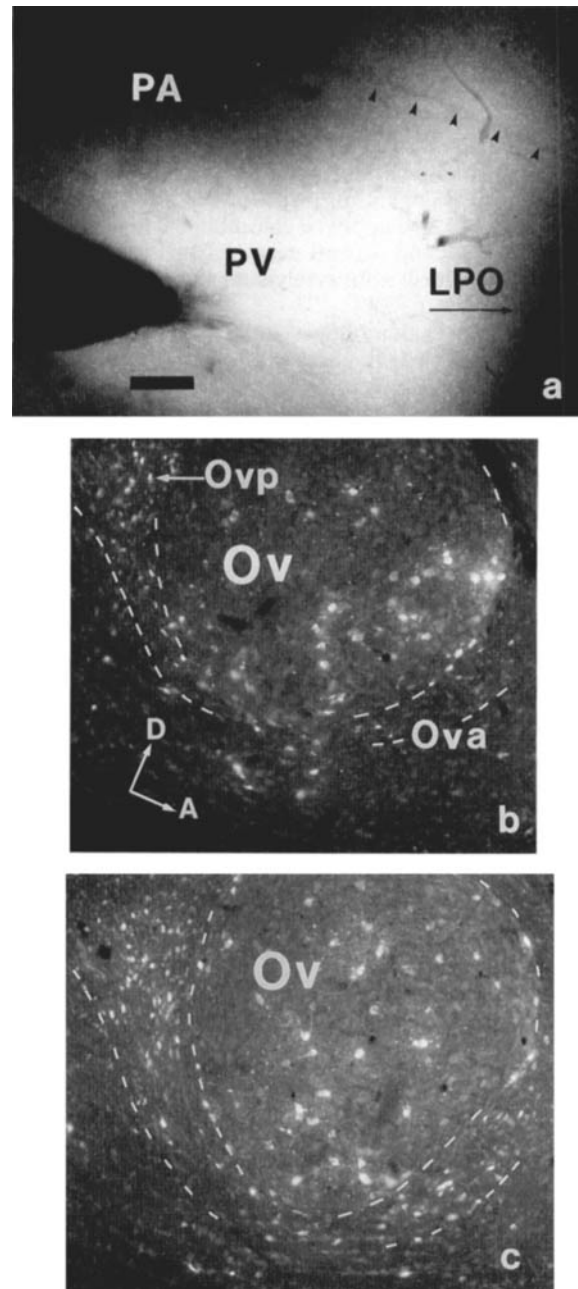

Fig. 19. An injection into PV and the edge of caudal LPO (a) resulted in some spread of the tracer into the lateral septum in sections medial to the level depicted here (ca. ML = 1.25). Arrows demarcate LMD. Labeled neurons were scattered within Ov proper as well as the shell (b and c), with Ovp containing relatively more label than Ova in this case. There appeared to be a slight increase in the distribution and density of label within both Ov and the shell along a medial (b) to lateral (c) progression. Scale bar, 250 μm in a and 100 μm in b and c.

ate distribution of labeled fibers. Minor projections were observed to the olfactory tubercle and lateral septum.

Functional considerations

Pathways that subserve polysensory convergence? The efferent connectivity of the Ov shell may subserve the integration of auditory input with other sensory systems.

In the budgerigar, Brauth et al. ('87) identified a projection from Ovm to a region laterally adjacent to field L. This laterally situated terminal field was also found by the authors to receive a visual projection from DLP. They argued that converging auditory and visual pathways within the lateral neostriatum might provide a neural substrate for intermodal associations important to individual recognition and social signalling within the budgerigar. This argument could also apply to columbids. The projection of the shell to the caudolateral neostriatum apparently overlaps with a similarly extensive visual projection field to this region (Güntürkün, '84).

An additional region of overlap between visual pathways and a target of the Ov shell is suggested by Wild ('87b). Wild's study in the pigeon revealed that a projection from the lateral perimeter of Ov, which may correspond to the pathway identified from Ovl to the anteroventral end-zone of L_2, overlapped with a projection from DLP onto this end-zone of the auditory neostriatum. Given that DLP is also a component of somatosensory pathways (Wild, '87b; Korzeniewska and Güntürkün, '90) and given that potentials evoked from cutaneous stimulation have been recorded from regions immediately anterior and medial to field L (Delius and Bennetto, '72), telencephalic efferents of the Ov shell may subserve the integration of auditory information with both visual and somatosensory input.

Projections to the lateral peripheray of the telencephalon from the shell suggest that this portion of the auditory thalamus could provide a source of converging auditory input to putative association areas of the avian telencephalon (Mogenson and Divac, '82; Reiner, '86). There is already some evidence that regions within the lateral telencephalon participate in auditory processing. Karten ('68) observed degenerating fibers within lateral neostriatum, archistriatum, and temporo-occipital corticoid areas (not included here as a shell target) subsequent to the lesion of Ov and its surround, but technical considerations rendered these findings inconclusive.

Regions of the lateral neostriatum in the budgerigar (e.g., NIVL) have been implicated as components of intratelencephalic pathways by Brauth and McHale ('88) and Brauth ('90). One of the sources of NIVL afferent fibers appeared to be the ventrolateral surround of Ov, depicted as extending to the border of DLP (Brauth and McHale, '88, cf. Fig. 4c). This region in the budgerigar may correspond to portions of the columbid Ov shell region (Ovl and Ovp) described here. Cytochrome oxidase histochemistry has implicated the lateral rim of the neostriatum as a possible site of auditory (and/or visual) activity, although staining was light in this region (Brauth, '90).

Wild et al. ('90) have shown that all portions of peri-Ov-SPO and peri-MLd-ICo receive input from the ventromedial archistriatum. These is evidence that implicates this region as a component of intratelencephalic auditory pathways (Wild et al., '90; Bonke et al., '79a). Conceivably, the Ov shell may receive feedback information from the telencephalon that could then feed forward onto the primary thalamo-telencephalic auditory pathway, from Ov to field L, given the efferent connectivity of the shell with Ov proper and the auditory neostriatum. Feedback from telencephalic processing could also influence hypothalamic areas mediating endocrine function via descending pathways from the Ov shell.

A putative interface between auditory and endocrine systems. There is correspondence of the Ov shell to an estrogen concentrating region that wraps around the ventral portion of Ov and extends away from the nucleus, along a lateral trajectory, within a region caudal to the auditory thalamus (Martinez-Vargas et al., '76, cf. Fig. 4g,h). If the Ov shell contains estrogen-concentrating neurons, its activity may be influenced by hormonal conditions. This influence could be concurrently transmitted to regions of "higher order" processing within the telencephalon and to the hypothalamus, where descending auditory pathways might provide a feedback system onto endocrine mediating regions (Cheng, '92).

One could reasonably ask why a descending projection from Ov has not been observed in previous studies of Ov efferents in the pigeon (Karten, '68), canary, *Serinus canaris,* (Kelley and Nottebohm, '79), the budgerigar (Brauth et al., '87), and the guinea fowl, *Numidea meleagris,* (Bonke et al., '79a). The latter three studies examined Ov efferents by using injections of tritiated amino acids into Ov. The nature of the descending pathway did not lend itself to visualization with this technique. Descending axons broke from the lateral forebrain bundle along several trajectories and across a wide area of the dorsal thalamus, with respect to its anteroposterior axis. No discrete fiber bundle was formed that would have permitted its ready discrimination by a technique relying upon relative differences in the density of a label instead of direct visualization of labeled axons. Additionally, since tissue is commonly analyzed in coronal sections, a projection that is dispersed along the anteroposterior axis is likely to be overlooked.

Descending projections to the hypothalamus from thalamic regions receiving midbrain auditory input have been reported for mammals (LeDoux et al., '85) and amphibians (Neary and Wilczynski, '86). In mammals, the descending projection to the ventromedial nucleus of the hypothalamus does not originate from the medial geniculate body itself, but from two nuclei immediately ventral to it that receive input from the shell of the inferior colliculus (LeDoux et al., '85). In amphibians, single unit recording within the ventral hypothalamus revealed neurons whose firing rate could be increased by presentation of either noise bursts or conspecific mating calls (Wilczynski and Allison, '89); Urano and Gorbman ('81) found that conspecific mating calls were more likely to stimulate excitatory responses in these regions than heterospecific calls.

The presence of a descending auditory pathway to hypothalamic regions involved in the control of steroid hormone levels raises the question of whether the neurons responsible for this projection preferentially respond to species-specific vocalizations. Preliminary results have suggested that single units within the shell respond in a complex manner to coo vocalizations. Activity of one recorded unit was evoked by only a single call type (the nest coo) of one sex (female) from a set of calls produced by both male and female doves (Durand et al., '90). Nest coo vocalizations are consistently performed over the course of several days at rates that can range up to 50 calls per hour (Miller, '89), thereby providing a tonic source of acoustic stimulation. Conceivably, this type of acoustic input could produce a tonic excitation or inhibition of specific neuronal populations within the posteromedial hypothalamus (including IH and caudal VMN), a region that mediates reproductive behavior (Gibson and Cheng, '79).

Unpublished data from our laboratory indicate a putative enkephalinergic projection from the Ov shell to the posteromedial hypothalamus (Cheng et al., '92). Given evidence

from the dove (Gibson and Cheng, '79) that the posteromedial hypothalamus mediates the performance of nest and copulation soliciation postures in the female, and evidence from mammals that enkephalin mediates a female solicitation posture (Pfaus and Gorzalka, '87), then comfirmation of an enkephalinergic auditory pathway to the hypothalamus would suggest a mechanism whereby courtship vocalizations influence reproductive behavior.

As previously observed, there is a striking overlap between much of the projection field of the Ov shell and regions of the avian brain that concentrate steroid or contain steroid receptors (Arnold et al., '76; Martinez-Vargas, '76; Balthazart et al., '89). A recently revealed estrogen concentrating region of the songbird brain, not seen in the dove, comprises the periventricular zone of the caudal neostriatum (Nordeen et al., '87; Gahr et al., '87). This region, NCm, was among the telencephalic targets of the Ov shell.

Implications for song learning species. The only established source of auditory input to the oscine song control system is field L_2 of the auditory neostriatum (Kelley and Nottebohm, '79), which projects to a peripherally located "shelf" of cells surrounding the song control nucleus originally designated the "caudal nucleus of the hyperstriatum ventrale" (HVc), a cell group necessary for song learning and production (Nottebohm et al., '76) and for female discrimination of song (Brenowitz, '91). Field L axons appear to contact only the dendrites of peripheral HVc neurons (Margoliash, '87), a surprisingly low level of input given that auditory activity is manifest not only in HVc (Zaretsky, '78; Katz and Gurney, '81) but also throughout the song system (Doupe and Konishi, '89; Williams and Nottebohm, '85).

The projection of the Ov shell region onto Nd and caudal HV, cell groups that have been proposed as possible evolutionary precursors of the oscine songbird HVc (Nottebohm et al., '76; Bonke et al., '79a), suggests that the question of thalamic auditory input to HVc should be re-examined. The HVc, recently redesignated as the high vocal center (HVC), is located in the dorsal pole of the caudal neostriatum of oscine songbirds and is thus comparable in its location to Nd. Pathways from the marginal zone of MLd to the dorsocaudal thalamus, the end-zone of the Ov shell, should also be examined in the songbird, given that the thalamic components of the avian song system reside within this portion of the thalamus (Okuhata and Saito, '87; Bottjer et al., '90).

In summary, a distinct region surrounding the nuclei ovoidalis and semilunaris parovoidalis has been demonstrated. The shell of the Ov-SPO complex was shown to receive a projection from the auditory midbrain, to contain acoustically responsive units, and to project to both telencephalic and non-telencephalic targets. The central auditory pathways examined in this report may serve to integrate auditory input with neuroendocrine activity and with polymodal processing, and may concurrently modulate activity within previously established auditory pathways associated with the n. ovoidalis.

ACKNOWLEDGMENTS

LITERATURE CITED

Akesson, T.R., N.C. DeLanerolle, and M.-F. Cheng (1987) Ascending vocalization pathways in the female ring dove: Projections of the nucleus intercollicularis. Exp. Neurol. 95:34–43.

Arnold, A.P., F. Nottebohm, and D.W. Pfaff (1976) Hormone concentrating cells in vocal control and other areas of the brain of the zebra finch (Poephila guttata). J. Comp. Neurol. 165:487–511.

Balthazart, J., M. Gahr, and C. Surlemont (1989) Distribution of estrogen receptors in the brain of the Japanese quail. Brain Res. 501:205–214.

Bell, P.M., D. Margoliash, and P.S. Ulinski (1989) Cytoarchitecture and differential projections of nucleus ovoidalis in the zebra finch. Soc. Neurosci. Abstr. 15:617.

Berk, M.L., and A.B. Butler (1981) Efferent projections of the medial preoptic nucleus and medial hypothalamus in the pigeon. J. Comp. Neurol. 203:379–399.

Bigalke-Kunz, B., R. Rubsamen, and G.J. Dorrscheidt (1987) Tonotopic organization of the auditory thalamus in a songbird, the European starling. J. Comp. Physiol. 161:255–265.

Bonke, B.A., D. Bonke, and H. Scheich (1979a) Connectivity of the auditory forebrain nuclei in the guinea fowl (Numida meleagris). Cell Tissue Res. 200:101–121.

Bonke, D., H. Scheich, and G. Langner (1979b) Responses of units in the auditory neostriatum of the Guinea Fowl (Numidea meleagris) to species-specific calls and synthetic stimuli. J. Comp. Physiol. 132:243–255.

Bottjer, S.W., K.A. Halsema, S.A. Brown, and E.I. Miesner (1990) Axonal connections of a forebrain nucleus involved with vocal learning in Zebra Finches. J. Comp. Neurol. 279:312–326.

Brauth, S.E. (1990) Investigation of central auditory nuclei in the budgerigar with cytochrome oxidase histochemistry. Brain Res. 508:142–146.

Brauth, S.E., C.M. McHale, C.A. Brasher, and R.J. Dooling (1987) Auditory pathways in the budgerigar. I. Thalamo-telencephalic projections. Brain Behav. Evol. 30:174–199.

Brauth, S.E., and C.M. McHale (1988) Auditory pathways in the budgerigar. II. Intratelencephalic pathways. Brain Behav. Evol. 32:193–207.

Brauth, S.E., and Reiner, A. (1991) Calcitonin-gene related peptide is an evolutionary conserved marker within the amniote thalamo-telencephalic auditory pathway. J. Comp. Neurol. 313:227–239.

Brenowitz, E.A. (1991) Altered perceptions of species-specific song by female birds after lesions of a forebrain nucleus. Science 251:303–305.

Brockway, B.F. (1969) Roles of budgerigar vocalizations in the integration of breeding behavior. In R.A. Hinde (ed): Bird Vocalizations. London and New York: Cambridge University Press, pp. 131–158.

Brzoska, J., and H.-J. Obert (1980) Acoustic signals influence the hormone production of the testes in the grass frog. J. Comp. Physiol. 140:25–29.

Cheng, M.-F. (1986) Female cooing promotes ovarian development in ring doves. Physiol. Behav. 37:371–374.

Cheng, M.-F., C. Desidero, M. Havens, and A. Johnson (1988) Behavioral stimulation of ovarian growth. Horm. Behav. 22:388–401.

Cheng, M.-F. (1992) For whom does the female dove coo? A case for the role of vocal self-stimulation. Anim. Behav., 43:1035–1044.

Cheng, M.-F., M.X. Zuo, S. Zhou, and S.E. Durand (1992) A subdivision of the avian central auditory system associated with met-enkephalin immunoreactivity. Third International Congress of Neuroethology, McGill University, Montreal, Canada.

Cohen, J., and M.-F. Cheng (1979) Role of vocalizations in the reproductive cycle of ring doves (Streptopelia risoria): Effects of hypoglossal nerve section on the reproductive behavior and physiology of the female. Horm. Behav. 13:113–127.

Cohen, J., and M.-F. Cheng (1981) The role of the midbrain in courtship behavior of the female ring dove (Streptopelia risoria): Evidence from radiofrequency lesion and hormone implant studies. Brain Res. 207:289–301.

Delius, J.D., and K. Bennetto (1972) Cutaneous sensory projections to the avian forebrain. Brain Res. 37:205–221.

Doupe, A.J., and M. Konishi (1989) Auditory properties of song nuclei of estrilid finches. Soc. Neurosci. Abstr. 15:347.

Durand, S.E., Cheng, M.-F., and J.M. Tepper (1989) Anatomical and electrical properties of the nucleus ovoidalis: Non-classical projections and single unit responses to species-specific calls. Soc. Neurosci. Abstr. 15:620.

Durand, S.E., Tepper, J.M., and M.-F. Cheng (1990) Acoustically responsive units in thalamic regions afferent to the basal ganglia. Soc. Neurosci. Abstr. 16:1250.

Fortune, E.S., and D. Margoliash (1991) Thalamic input and cytoarchitecture of auditory neostriatum in the Zebra Finch. Soc. Neurosci. Abstr. 17:446.

Gahr, M., G. Flugge, and H.-R. Guttinger (1987) Immunocytochemical localization of estrogen-binding neurons in the songbird brain. Brain Res. 402:173–177.

Gerfen, R.G., and P.L. Sawchenko (1984) An anterograde neuroanatomical tracing method that shows the detailed morphology of neurons, their transported plant lectin, Phaseolus vulgaris leucoagglutinin (PHA-L). Brain Res. 290:219–238.

Gibson, M.J., and M.-F. Cheng (1979) Neural mediation of estrogen-dependent courtship behavior in female ring doves. J. Comp. Physiol. Psych. 93:855–867.

Güntürkün, O. (1984) Evidence for a third visual area in the telencephalon of the pigeon. Brain Res. 294:247–254.

Hausler, U. (1988) Topography of the thalamotelencephalic projections in the auditory system of a songbird (Sternus vulgaris). In J. Syka and B. Masterton (eds): Auditory Pathway: Structure and Function. London: Plenum Press, pp. 197–202.

Hsu, S.-M., L. Raind, and H. Fauser (1981) Use of avidin-biotin-peroxidase complex (ABC) in immunoperoxidase technique. J. Histochem. Cytochem. 29:577–580.

Itoh, K., A. Konishi, S. Nomura, N. Mizuno, Y. Nakamura, and T. Sugimoto (1979) Application of coupled oxidation reaction to electron microscopic demonstration of horseradish peroxidase: cobolt-glucose oxidase method. Brain Res. 175:341–436.

Izzo, P.N. (1991) A note on the use of biocytin in anterograde tracing studies in the central nervous system: Application at both light and electron microscopic level. J. Neurosci. 36:155–166.

Karten, H.J. (1967) The organization of the ascending auditory pathway in the pigeon (Columba livia). I. Diencephalic projections of the inferior colliculus (nucleus mesencephali lateralis, pars dorsalis). Brain Res. 6:409–427.

Karten, H.J. (1968) The ascending auditory pathway in the pigeon (Columbia livia). II. Telencephalic projections of the nucleus ovoidalis thalami. Brain Res. 11:134–153.

Karten, H.J., and W. Hodos (1967) A Stereotaxic Atlas of the Brain of the Pigeon (Columbia livia). Baltimore: Johns Hopkins Press.

Katz, L.C., and M.E. Gurney (1981) Auditory responses in the zebra finch's motor system for song. Brain Res. 211:192–197.

Kelley, D.B., and F. Nottebohm (1979) Projections of a telencephalic auditory nucleus—Field L—in the canary. J. Comp. Neurol. 183:455–470.

King, M.A., P.M. Louis, B.E. Hunter, and D.W. Walker (1989) Biocytin: A versatile anterograde neuroanatomical tract-tracing alternative. Brain Res. 497:361–367.

Kitt, C.A., and S.E. Brauth (1981) Projections of the paleostriatum upon the midbrain tegmentum in the pigeon. Neuroscience 6:1551–1566.

Korzeniewska, E., and O. Güntürkün (1990) Sensory properties and afferents of the nucleus dorsolateralis posterior thalami of the pigeon. J. Comp. Neurol. 292:457–479.

Kroodsma, D.E. (1976) Reproductive development in a female songbird: Differential stimulation by quality of male song. Science 192:574–575.

Kudo, M., and K. Niimi (1980) Ascending projections of the inferior colliculus in the cat: An autoradiographic study. J. Comp. Neurol. 191:545–556.

Kuenzel, W.J., and M. Masson (1988) A stereotaxic atlas of the brain of the chick (Gallus domesticus). Baltimore: Johns Hopkins Press.

LeDoux, J.E., D.A. Ruggeiro, and D.J. Reis (1985) Projections to the subcortical forebrain from anatomically defined regions of the medial geniculate body in the rat. J. Comp. Neurol. 242:182–213.

Liebler, L.M. (1975) Monoaural and Binaural Pathways in the Ascending Auditory System of the Pigeon. Ph.D. thesis, Department of Psychology, Massachusetts Institute of Technology, Cambridge.

Margoliash, D. (1987) Neural plasticity in birdsong learning. In J.P. Rauschecker and P. Marler (eds): Imprinting and Cortical Plasticity. New York. Wiley, pp. 23–54.

Martinez-Vargas, M.C., W.E. Stumpf, and M. Sar (1976) Anatomical distribution of estrogen target cells in the avian CNS: A comparison with the mammalian CNS. J. Comp. Neurol. 167:83–104.

McComb, K. (1987) Roaring in red deer stags advances the date of oestrus in hinds. Nature 330:648–649.

Miller, H. (1989) Afferent projections of the nucleus taenia and its role in the courtship behavior of ring doves, Streptopelia risoria. Unpub. Masters thesis, Rutgers University, Graduate School Newark.

Mogensen, J., and I. Divac (1982) The prefrontal "cortex" in the pigeon: Behavioral evidence. Brain Behav. Evol. 21:60–66.

Neary, T.J., and W. Wilcznski (1986) Auditory pathways to the hypothalamus in ranid frogs. Neurosci. Lett. 71:142–147.

Nordeen, K.W., E.J. Nordeen, and A.P. Arnold (1987) Estrogen accumulation in zebra finch song control nuclei: Implications for sexual differentiation and adult activation of song behavior. J. Neurobiol. 18:569–582.

Nottebohm, F., and M.E. Nottebohm (1971) Vocalizations and breeding behavior of surgically deafened ring doves (Streptopelia risoria). Anim. Behav. 19:313–327.

Nottebohm, F., T.M. Stokes, and C.M. Leonard (1976) Central control of song in the canary, Serinus canarius. J. Comp. Neurol. 165:457–486.

Okuhata, S., and N. Saito (1987) Synaptic connections of thalamo-cerebral vocal nuclei in the canary. Brain Res. Bull. 18:35–44.

Pfaus, J.G. and B.B. Gorzalka (1987) Selective activation of opioid receptors differentially affects lordosis behavior in female rats. Peptides 8:309–317.

Reiner, A. (1986) Is prefrontal cortex found only in mammal? Trends Neurosci. 9:298–300.

Rose, M. (1914) Uber die cytoarchitectonische Gliederung des Vorderhirns der Vogel. J. Psychol. Neurol. (Lpz) 21:278–352.

Shu, S., G. Ju, and L. Fan (1988) The glucose-oxidase-DAB-nickel method in peroxidase histochemistry of the nervous system. Neurosci. Lett. 85:169–171.

Shu, S.Y., and G.M. Peters (1988) Anterograde and retrograde axonal transport of Phaseolus vulgaris leucoagglutinin (PHA-L) from the globus pallidus to the striatum of the rat. J. Neurosci. Methods 25:175–180.

Urano, A., and A. Gorbman (1981) Effects of pituitary hormonal treatment on responsiveness of anterior preoptic neurons in male leopard frogs (Rana pipiens). J. Comp. Physiol. 141:163–171.

Vowles, D.M., L. Beazley, and D.H. Harwood (1975) A stereotaxic atlas of the brain of the Barabary Dove. In P. Caryl and D.M. Vowles (eds): Neural and Endocrine Aspects of Behavior in Birds. Amsterdam: Elsevier Scientific Publishing Co., pp. 351–394.

Wilczynski, W., and J.D. Allison (1989) Acoustic modulation of neural activity in the hypothalamus of the leopard frog. Brain Behav. Evol. 33:317–324.

Wild, J.M. (1987a) Nuclei of the lateral lemniscus project directly to the thalamic auditory nuclei in the pigeon. Brain Res. 408:303–307.

Wild, J.M. (1987b) The avian somatosensory system: Connections of regions of the body representation in the forebrain of the pigeon. Brain Res. 412:205–223.

Wild, J.M., B.J. Frost, and H.J. Karten (1990) Some aspects of the organization of the auditory forebrain and midbrain in the pigeon. Soc. Neurosci. Abstr. 16:715.

Williams, H., and F. Nottebohm (1985) Auditory responses in avian vocal motor neurons: A motor theory for song perception in birds. Science 229:279–282.

Zaretsky, M.D. (1978) A new auditory area of the songbird forebrain: A connection between auditory and song control centers. Exp. Brain Res. 32:267–273.